



**Technische Universität München**

**Klinik und Poliklinik für Chirurgie, Klinikum rechts der Isar**

**Angiocrine HGF signalling controls physiologic organ and body size and dynamic  
hepatocyte proliferation to prevent liver damage during regeneration**

**Xuejun Zhang**

Vollständiger Abdruck der von der Fakultät für Medizin der Technischen Universität  
München zur Erlangung des akademischen Grades eines

Doktors der Medizin (Dr. med.)

genehmigten Dissertation.

Vorsitzender: Prof. Dr. Jürgen Schlegel

Prüfer der Dissertation:

1. Priv.-Doz. Dr. Norbert Hüser

2. Priv.-Doz. Dr. Carolin Mogler

Die Dissertation wurde am 25.04.2019 bei der Technischen Universität  
München eingereicht und durch die Fakultät für Medizin am 13.08.2019  
angenommen.

Part of this thesis was submitted for publication at the time of thesis submission.

Parts of this thesis were presented at the following scientific conferences:

### **1. Electronic scientific poster presentation**

Conference name: 13th World Congress of the International Hepato-Pancreato-Biliary Association 2018

Conference organizer: International Hepato-Pancreato-Biliary Association

Conference date: 4-7 September 2018

Conference place: Geneva, Switzerland

Title: Hepatic angiocrine HGF signalling plays a vital role in the early stage of liver regeneration after PHx in mice.

Presenting author: Xuejun Zhang

### **2. Scientific poster presentation.**

Conference name: UEG Week Vienna 2018

Conference organizer: United European Gastroenterology

Conference date: 23 October 2018

Conference place: Vienna, Austria

Title: Hepatic angiocrine HGF signalling plays a crucial role in the early stage of liver regeneration after partial hepatectomy in mice

Presenting author: Xuejun Zhang

### **3. Scientific poster presentation.**

Conference name: Kongress der Deutschen Gesellschaft für Chirurgie 2019

Conference organizer: Deutsche Gesellschaft für Chirurgie

Conference date: 28 March 2019

Conference place: Munich, Germany

Title: Der HGF-Signalweg spielt eine bedeutende Rolle in frühen Stadien der Leberregeneration nach partieller Hepatektomie

Presenting author: Xuejun Zhang

# Table of Contents

<b>Technische Universität München</b> .....	0
<b>Abstract</b> .....	6
<b>1 Introduction</b> .....	8
1.1 The functions and physiology of the liver .....	8
1.2 Liver regeneration after liver injury .....	10
1.3 Liver hypertrophy in liver regeneration.....	11
1.4 Regulation of liver regeneration by growth factors and cytokines .....	12
1.5 Mouse models in liver regeneration .....	16
1.6 The role of HGF in liver regeneration .....	17
1.7 HGF/c-Met signalling pathway gene knockout mouse models in liver regeneration .....	18
<b>2 Aims of the study</b> .....	20
<b>3 Materials and methods</b> .....	21
3.1 Materials.....	21
3.1.1 Chemicals and reagents .....	21
3.1.2 Antibodies.....	23
3.1.3 Laboratory equipments .....	24
3.1.4 Kits.....	25
3.1.5 Buffers and solutions.....	26

3.2 Methods.....	28
3.2.1 Generation of HGF <sup>ALSEC</sup> mouse model.....	28
3.2.2 Partial hepatectomy.....	28
3.2.3 Preparation for paraffin-embedded liver sections .....	29
3.2.4 Immunohistochemistry .....	29
3.2.5 Hematoxylin & eosin (H&E) staining.....	30
3.2.6 Periodic acid-Schiff (PAS) staining.....	30
3.2.7 Image processing .....	31
3.2.8 RNA isolation from liver tissue .....	31
3.2.9 Complementary DNA reverse transcription.....	33
3.2.10 Quantitative reverse-transcription PCR (qRT-PCR).....	34
3.2.11 DNA isolation from mouse tails.....	36
3.2.12 Genotyping .....	36
3.2.13 Protein extraction from liver tissue.....	37
3.2.14 Protein detection and quantitation .....	38
3.2.15 Western blotting.....	38
3.2.16 ELISA.....	39
3.2.17 RNA sequencing.....	40
3.3 Statistics.....	41
<b>4 Results.....</b>	<b>42</b>
4.1 HGF ablation in LSECs results in reduced organismal growth but normal liver development.....	42

4.2 Liver regeneration is compromised in HGF <sup>ALSEC</sup> mice.....	45
4.3 Lethality of HGF <sup>ALSEC</sup> mice is higher than control mice after PH .....	49
4.4 Liver necrosis in HGF <sup>ALSEC</sup> mice is more visible after PH .....	49
4.5 Serum ALT levels of HGF <sup>ALSEC</sup> are elevated after PH .....	52
4.6 HGF mRNA expression of whole liver lysates is downregulated during liver regeneration .....	53
4.7 HGF/c-Met signalling pathway is impaired in HGF <sup>ALSEC</sup> mice after PH .....	54
4.8 Deptor protein is downregulated in HGF <sup>ALSEC</sup> mice after PH .....	57
5.1 The generation of a new LSEC-specific HGF KO mouse model .....	59
5.2 Ablation of HGF in LSECs results in lower body weight but normal liver development and function.....	60
5.3 Ablation of HGF in LSECs suppresses liver regeneration at the early stage after PH .....	61
5.4 The mechanisms of impaired liver regeneration in HGF <sup>ALSEC</sup> mice.....	62
5.5 Liver necrosis after PH in HGF <sup>ALSEC</sup> mice .....	64
5.6 LSEC and liver regeneration .....	65
<b>6 Summary .....</b>	<b>67</b>
<b>7 Abbreviations .....</b>	<b>68</b>
<b>8 Figures and tables .....</b>	<b>70</b>
8.1 Figures .....	70
8.2 Tables.....	71
<b>9 References .....</b>	<b>72</b>

10 Curriculum vitae .....	84
11 Acknowledgements .....	86

# Abstract

## Background:

Liver sinusoidal endothelial cells (LSECs) are highly specialised endothelial cells that control organ function, metabolism, and development through the secretion of so called angiokines. LSECs express hepatocyte growth factor (HGF), a complete hepatic mitogen that is required for prenatal development, involved in metabolic homeostasis, and is considered an initiator of liver regeneration. However, the exact contributions of LSECs derived HGF to the many functions of HGF remain to be defined.

## Methods:

Stab2-iCre<sup>tg/wt</sup>;HGF<sup>fl/fl</sup> (HGF<sup>ΔLSEC</sup>) mice were used to continuously abrogate HGF expression selectively in LSECs from early foetal development onwards. Global development, metabolic and endothelial zonation, and organ functions were assessed. To investigate liver regeneration, a 70% partial hepatectomy (PH) was performed. The kinetics of liver-to-body weight ratio, hepatocyte proliferation, and the HGF/c-MET signalling pathway were then analysed at different time points after PH.

## Results:

HGF<sup>ΔLSEC</sup> mice were viable and fertile. Although metabolic and endothelial zonation as well as the liver to body weight ratio were not altered, total body weight and total liver weight were reduced in HGF<sup>ΔLSEC</sup> compared to control mice. Necrotic organ damage was more marked in HGF<sup>ΔLSEC</sup> and regeneration was delayed 72 h after PH. This was associated with decreased hepatocyte proliferation at 48 h after PH. The HGF/c-MET signalling pathway was less active in HGF<sup>ΔLSEC</sup> than in control mice and impaired activation of this axis involved downregulation of the anti-apoptotic protein Deptor, representing a novel target of this signalling pathway in this context.

**Conclusions:**

Angiocrine HGF is involved in the control of body and organ growth as well as the early stages of liver regeneration after PH to prevent excessive organ damage.

# 1 Introduction

## 1.1 The functions and physiology of the liver

The liver is the biggest solid glandular organ in humans which provides a multitude of essential functions for the whole body. The liver plays a vital role in immunity, drug detoxification, and digestion. It is also important for metabolism, including glycogen storage, plasma protein synthesis, and vitamin storage.

The liver mass comprises approximately 2%–5% of the body weight.(Si-Tayeb, Lemaigre et al. 2010) It can be divided into four sections (the right anterior section, right posterior section, left medial section, and left lateral section) and eight anatomical segments(Liau, Blumgart et al. 2004) (Figure 1A, 1B). The basic functional unit of the liver is the liver lobule. It comprise plates of hepatocytes lined by sinusoidal capillaries that radiate towards the central vein. Liver lobules are surrounded by a portal triad of vessels consisting of a portal vein, bile duct, and hepatic artery(Si-Tayeb, Lemaigre et al. 2010) (Figure 2). Both the portal vein and hepatic artery flow through a network of sinusoidal capillaries to the central vein.

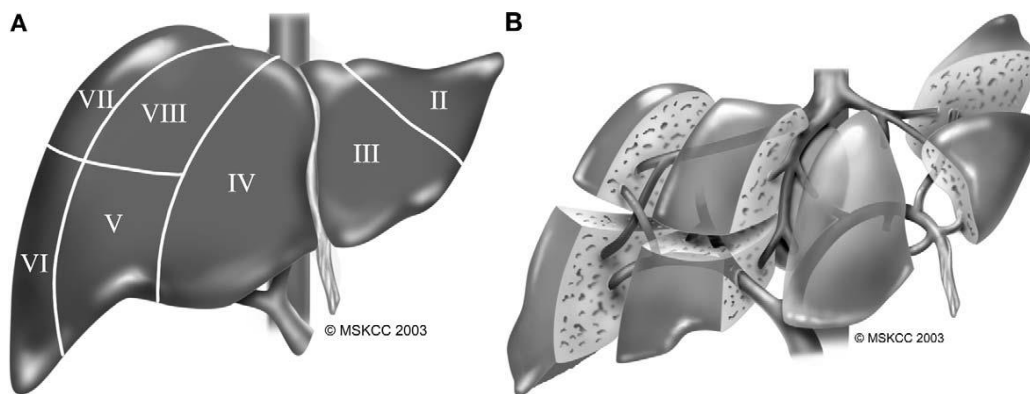


**Figure 1.** Liver lobes and segments.(Liau, Blumgart et al. 2004) **A.** The eight segments of the liver. **B.** Each of the liver segments has an independent portal venous supply and hepatic arterial supply. Segment I is not shown.

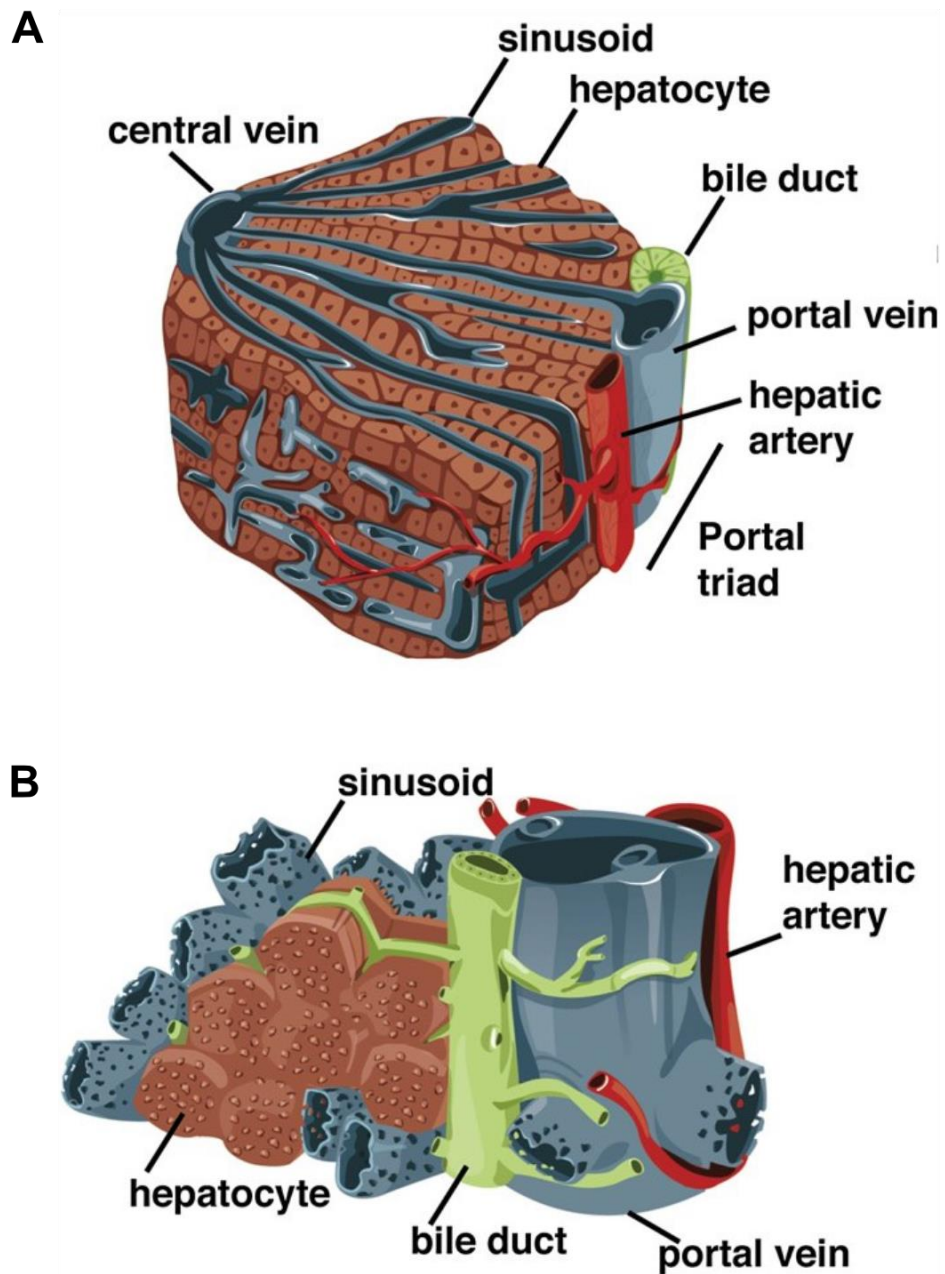


**Figure 2.** The structure of the liver.(Si-Tayeb, Lemaigre et al. 2010) **A.** The lobule structure. **B.** The relationship between key cellular compartments of the liver.

The majority of liver is hepatocytes, which constitute 78% of the parenchymal volume; the remaining parts of the liver consist of 2.8% endothelial cells, 2.1% Kupffer cells, and 1.4% fat-storing cells.(Blouin, Bolender et al. 1977)

The hepatic artery supplies 25% well-oxygenated blood, while the hepatic portal vein supplies 75% of the blood to the liver, which is deoxygenated venous blood.(Saxena, Theise et al. 1999, Eipel, Abshagen et al. 2010) The liver receives blood circulation through the portal vein from the small and large intestines, as well as the spleen and pancreas. During this process, nutrients are absorbed from the intestine and synthesised into all kinds of proteins, which control osmotic balance and hormone delivery. Lipids are sent as lipoproteins to other tissues. The liver acts as a reservoir for the nutritional and energy needs of the body. For example, carbohydrates are stored in the liver as glycogen, which is the main glucose reserve used to stabilise blood glucose levels. Thus, the liver plays crucial roles in metabolic homeostasis. Additionally, the liver detoxifies toxins and xenobiotics to keep the body healthy.(Michalopoulos 2007, Michalopoulos 2013)

## **1.2 Liver regeneration after liver injury**

Since the liver has many vital functions, the size of the liver needs to be properly adjusted to provide for the needs of the body, which has been described by the term “hepatostat”.(Michalopoulos 2013, Michalopoulos 2017) The liver expands in size to meet the physiological needs of the body (e.g. during pregnancy, and growth during childhood and adolescence). In contrast, the liver decreases in size in response to disease (cachexia, responses to chemotherapy, and chronic inflammatory conditions).(Michalopoulos 2013)

Liver regeneration is necessary to maintain normal liver function after liver injury. The liver contains two types of epithelial cells, hepatocytes and cholangiocytes (also known as biliary epithelial cells). Liver sinusoid endothelial cells (LSECs) line hepatic capillaries, with macrophages (Kupffer

cells) interspersed along the sinusoid lumen. Hepatic stellate cells (HSCs) exist between sinusoids and hepatocytes.(Michalopoulos and Khan 2015)

All hepatic cell types are involved in the regenerative process, without the participation of stem cells or progenitor cells.(Michalopoulos 2007, Michalopoulos 2013, Michalopoulos 2014) Hepatocytes are the first to proliferate after liver injury, which is followed by the proliferation of HSCs, cholangiocytes, Kupffer cells, and LSECs.(Michalopoulos 2007) The proliferation of hepatocytes starts in the periportal to pericentral areas of the liver lobule. Hepatocytes surrounding the central veins enter mitoses last.(Gebhardt, Baldysiak-Figiel et al. 2007) Cholangiocytes proliferate a little later after the hepatocytes. Proliferation of LSECs starts at 2–3 d and terminates approximately 4–5 d after PH.(Michalopoulos 2007)

An interesting phenomenon is that hepatocytes and cholangiocytes can act as facultative stem cells for each other.(Poisson, Lemoine et al. 2017) When the regenerative capacity of hepatocytes is compromised, the cholangiocytes can function as facultative stem cells that transdifferentiate into hepatocytes. Conversely, in situations when the proliferative capacity of cholangiocytes is compromised, the periportal hepatocytes can function as facultative stem cells and transdifferentiate to cholangiocytes.(Michalopoulos and Khan 2015, Poisson, Lemoine et al. 2017)

### **1.3 Liver hypertrophy in liver regeneration**

The liver is an interesting organ with a high regenerative capacity. Human liver restoration after partial hepatectomy is achieved not only by replication of various types of hepatic cells, but also by an increase in cell size.(Clavien, Petrowsky et al. 2007) Hepatocyte proliferation generally starts within 1 d after a major resection of the human liver.(Clavien, Petrowsky et al. 2007) Several reports have shown hypertrophy of hepatocytes in the regenerated liver in the mouse.(Haga, Ogawa et al. 2005, Haga, Ozaki et al. 2009, Miyaoka, Ebato et al. 2012) The liver regenerates from 30% PH by hypertrophy of the

hepatocytes without proliferation. However, in 70% PH, hypertrophy occurs first and then cell division follows to increase the cell number. After 70% PH, the size of the hepatocytes increases slightly as early as 3 h, peaks at 1 d, and then gradually decreases.(Miyaoaka, Ebato et al. 2012) During liver regeneration after 70% PH, the number of hepatocytes increases by 1.6-fold, and the volume of hepatocytes increases by 1.5-fold. Taken together, the number and volume increases result in approximately a 2.4-fold increase in liver weight.(Miyaoaka, Ebato et al. 2012)

#### **1.4 Regulation of liver regeneration by growth factors and cytokines**

Most hepatic cells proceed from G1 to S phase of the cell cycle after liver injury. Figure 3 (modified from reference 17) shows regulation of the G1/S transition.(Sherr and Roberts 1999) Activation of cyclins and cyclin-dependent kinases cooperatively regulate hepatic cell proliferation. D-type cyclins act as growth factor sensors. Cyclin Ds (D1, D2, and D3) assemble with their catalytic partners, CDK4 and CDK6, as cells progress through G1 phase. Sequestration of Cip/Kip proteins activate the Cyclin E–CDK2 complex. CDK4 and CDK6 contribute to Rb phosphorylation, facilitate E2F family members, and activate the genes required for entry into S phase. CDK2 and Cyclins E and A can regulate nucleotide metabolism and DNA synthesis.

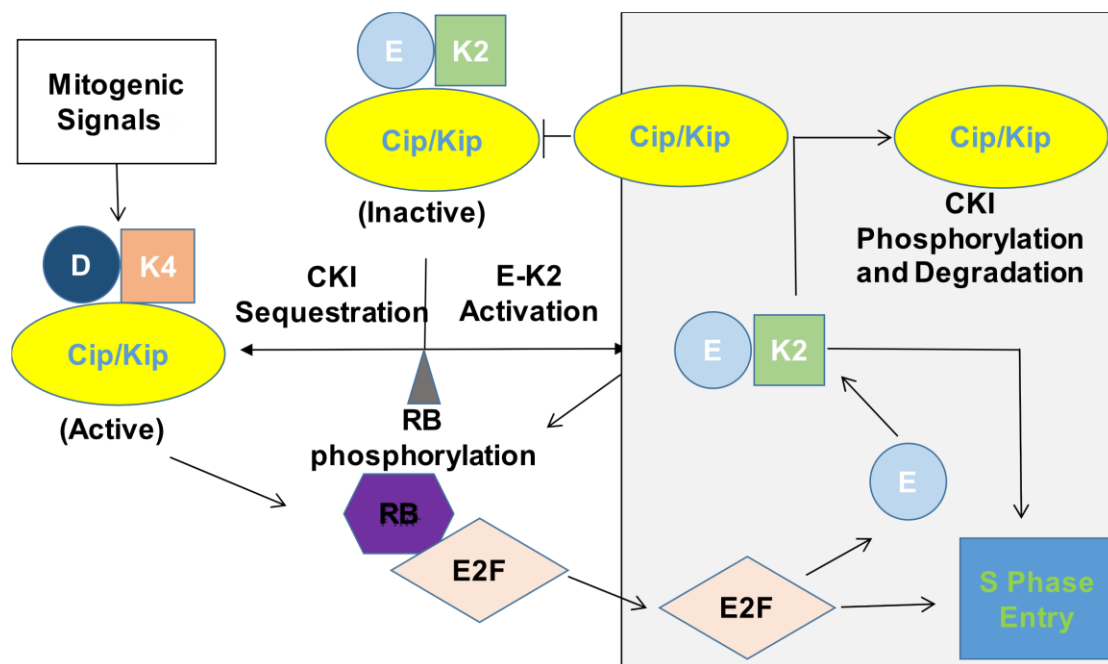


**Figure 3.** Regulation of the G1/S transition.(Sherr and Roberts 1999)

Many cytokines and growth factors are involved during the liver regeneration process.(Sherr and Roberts 1999, Costa, Kalinichenko et al. 2003) Transcription factors, e.g. C/EBP $\alpha$  and  $\beta$ , Signal transducer and activator of transcription 3 (STAT3), and nuclear factor  $\kappa$ B (NF- $\kappa$ B) are also involved. Recently, our research group found that MAVS(Schulze, Stoss et al. 2018) and Brg1(Wang, Kaufmann et al. 2019) proteins can also affect liver regeneration through the regulation of cell cycle.

Proliferative events after PH are initiated and controlled by complete mitogens and incomplete mitogens.(DeLeve 2013) HGF proliferative events after PH are initiated and controlled by complete mitogens and auxiliary mitogens. Complete mitogens are mitogenic in hepatocyte cultures and can also induce liver enlargement when injected into live animals. Currently there are two groups of complete mitogens. The first group includes HGF and its receptor c-Met. The other group includes epidermal growth factor receptor (EGFR) and its ligands EGF, transforming growth factor alpha (TGF-alpha), amphiregulin, and HB-EGF.(Mitchell, Nivison et al. 2005, Michalopoulos 2010, Michalopoulos

2013) HGF performs its activity through the activation of the receptor tyrosine kinase c-Met. The HGF/c-Met signalling pathway plays a vital role during liver regeneration. EGFR signalling is also important, but not essential, for liver regeneration.(Bohm, Kohler et al. 2010) There is upregulation of (TGF)- $\alpha$ , HB-EGF, and amphiregulin after PH.(Michalopoulos 2007)

Auxiliary mitogens are signals whose deprivation delays but does not abolish liver regeneration. These signals are not mitogenic in primary cultures of hepatocytes and administration of these auxiliary mitogens to animals does not lead to liver enlargement. Elimination of any of these signals delays, but does not terminate, liver regeneration. Auxiliary mitogens include TNF, IL-6, norepinephrine, Notch and Jagged, vascular endothelial growth factor (VEGF), the gene encoding insulin-like growth factor binding protein (IGFBP), bile acids, serotonin, complement, leptin, oestrogens, and fibroblast growth factors (FGF1 and FGF2).(Bohm, Kohler et al. 2010, Michalopoulos 2013)

There is no single signal driving liver regeneration. As shown in Figure 4, many growth factors and cytokines from different hepatic cell types interact with each other during liver regeneration.(Michalopoulos 2007)

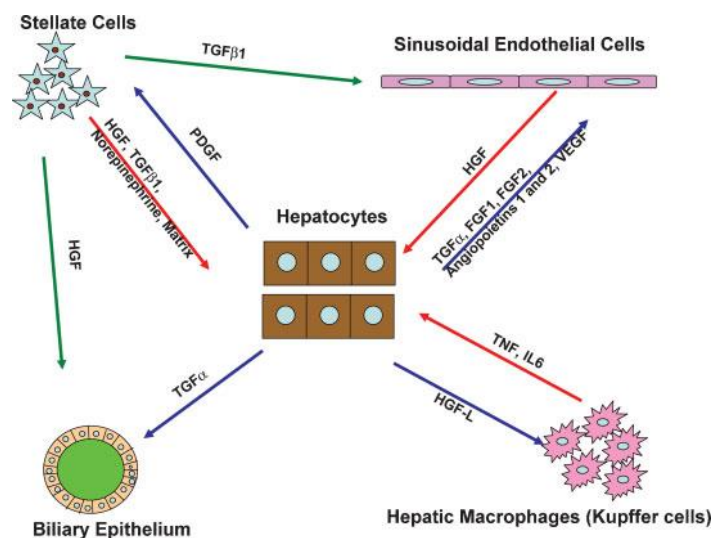


**Figure 4.** Signalling interactions between different hepatic cell types during liver regeneration. (Michalopoulos 2007).

A list of the most studied signals associated with the initiation of hepatocyte proliferation is provided below.(DeLeve 2013)

<b>Hepatic mitogens</b>	
<b><i>Complete mitogens</i></b>	<b><i>Incomplete mitogens</i></b>
HGF	VEGF
EGF	FGF1
TGF- $\alpha$	FGF2
Heparin-binding EGF	Notch
Amphiregulin	Jagged
	Complement proteins
	Leptin
	Insulin
	Norepinephrine
	TNF
	IL-6
	TGF- $\beta$
	Bile acids
	Serotonin
	Hyaluronic acid
	Wnt2

## 1.5 Mouse models in liver regeneration

Regeneration after the loss of liver tissue is a fundamental response of the liver to injury. Loss of hepatic tissue can be induced by hepatotoxic chemicals (e.g. CCl<sub>4</sub>). The events of the first day after toxic injury are dominated by acute inflammation of the necrotic zones, when macrophages and leukocytes migrate to the necrotic area to remove dead hepatocytes. After that, the regenerative response follows.

A two thirds partial hepatectomy (PH) is the mostly studied experimental model for liver regeneration. The left and median lobes of the liver, which comprise approximately two thirds of the organ, are surgically removed. Consequently, the normally quiescent and highly differentiated liver cells begin to proliferate and the original liver mass is restored within 7–10 d (in rodents) by regeneration of the residual liver tissue. Claudia et al. (Mitchell and Willenbring 2008) produced a protocol which is a reproducible and well-tolerated method for a two thirds partial hepatectomy in mice.

The PH model has two advantages that make it so popular. (Michalopoulos 2010) Firstly, the removal of the resected liver is not accompanied by massive inflammation or necrosis, is relatively clean, and does not induce liver fibrosis. Thus, liver regeneration of the residual lobes is only induced by processes relevant to liver tissue and not to necrosis or acute inflammation. In contrast, models induced by hepatotoxic chemicals produce an inflammatory response that removes tissue debris. Secondly, the regenerative process can be precisely timed, and PH can be performed in standard conditions within approximately 20 min by an experienced surgeon. Therefore, many investigators have used the PH model to research liver regeneration over the years.

## 1.6 The role of HGF in liver regeneration

Hepatocyte growth factor (HGF) is a complete hepatic mitogen and is considered an initiator of liver regeneration.(Michalopoulos 2010, Michalopoulos 2013) C-Met is the unique receptor for HGF and is expressed in the epithelial cells of many organs, including the liver, pancreas, kidney, etc. HGF/c-Met is involved in numerous signalling pathways, including proliferation, motility, migration, and invasion.(Organ and Tsao 2011) The HGF/c-Met signalling pathway is fundamental for normal hepatocyte function and liver regeneration. HGF was first isolated from rat serum after partial hepatectomy, and its function was therefore associated with liver regeneration.(Nakamura, Nawa et al. 1984, Russell, McGowan et al. 1984) Nowadays, it is known that HGF can be secreted by different cell types of mesenchymal origin in various organs, such as the lung, liver, brain, thyroid, and salivary gland.(Lindroos, Zarnegar et al. 1991, Fajardo-Puerta, Mato Prado et al. 2016)

HGF was identified by two independent studies as both a motility factor and a scatter factor for hepatocytes, and later this factor was found to be the same molecule.(Stoker, Gherardi et al. 1987, Nakamura, Nishizawa et al. 1989, Weidner, Arakaki et al. 1991) HGF acts as a pleiotropic factor and a cytokine, promoting cell proliferation, survival, motility, scattering, differentiation, and morphogenesis.(Organ and Tsao 2011)

HGF is secreted by mesenchymal cells as a single-chain, biologically inert precursor (pro-HGF) and is stored in the extracellular matrix. Pro-HGF is processed into its bioactive form when extracellular proteases cleave the bond between Arg494 and Val495. Hepatocyte growth factor-activator and matriptase are the main proteases responsible for the processing of HGF. The mature form of HGF is a disulphide-linked heterodimer, which consists of an  $\alpha$ -chain and  $\beta$ -chain.(Basilico, Arnesano et al. 2008, Trusolino, Bertotti et al. 2010, Organ and Tsao 2011) After binding to its tyrosine kinase receptor, c-Met, dimerisation and phosphorylation of the C-terminal receptor domain ensues,

leading to interactions with multiple signal transducers, such as STAT3, GRB-2, SHC, or PLC $\gamma$ .(Migliore and Giordano 2008, Giordano and Columbano 2014)

As early as 2 h after PH, the HGF protein concentration in the plasma rises more than 10-fold.(Lindroos, Zarnegar et al. 1991) At 3 h after PH, HGF mRNA levels start to rise in the liver and peak 12 h after PH.(Zarnegar, DeFrances et al. 1991)

### **1.7 HGF/c-Met signalling pathway gene knockout mouse models in liver regeneration**

Constitutive and global knockouts (KO) of HGF and c-Met in mice are lethal during development between E12.5 and E16.5, with HGF KO embryos showing a severely reduced liver size.(Bladt, Riethmacher et al. 1995, Schmidt, Bladt et al. 1995) In the adult liver, HGF is expressed by Kupffer cells, HSCs, and LSECs.(Noji, Tashiro et al. 1990, Maher 1993) After liver damage, HGF gene expression shows an upregulation exclusively in endothelial cells.(Maher 1993) Previous studies have shown that LSECs secrete several hepatotropic proteins, such as HGF, BMP2, wnt9b, and wnt2 to stimulate liver regeneration and control metabolic functions.(LeCouter, Moritz et al. 2003, Ding, Nolan et al. 2010, Koch, Olsavszky et al. 2017, Leibing, Geraud et al. 2018) Such endothelial cell-derived paracrine acting factors are also known as angiocrine factors or angiokines.(Rafii, Butler et al. 2016) Although angiocrine Bmp2 and wnt signalling pathways have been shown to control whole body iron metabolism and metabolic liver zonation, respectively, under steady state conditions,(Koch, Olsavszky et al. 2017, Leibing, Geraud et al. 2018) HGF and wnt2 have been shown to induce hepatocyte proliferation after PH.(Ding, Nolan et al. 2010)

Since the constitutive KO of HGF or c-Met in mice is lethal during development, inducible KO mice have been generated to study the functions of these proteins during regeneration. The inducible knockout of hepatocyte-specific c-Met in adult mice does not compromise physiological liver function or structure.

However, these mice die 48 h after PH and exhibit liver necrosis and diffuse macro- or microvesicular steatosis, indicating that c-Met activation is required for liver regeneration but not physiological maintenance of hepatic functions in adult mice.(Huh, Factor et al. 2004)

## 2 Aims of the study

To study endothelium derived HGF in adult mice, partial hepatectomy (PH) was performed on mice with an endothelial specific tamoxifen-induced vascular endothelial (VE)–cadherin-Cre-mediated deletion of HGF. After PH, these mice indeed showed increased lethality, reduced hepatocyte proliferation, enhanced collagen deposition, and increased cell apoptosis compared to control mice, indicating that upregulation and secretion of HGF by LSECs during regeneration cannot be compensated for by other HGF-expressing cells.<sup>49</sup> Although it was not specifically reported in this publication, these mice appeared to have normal physiological liver functions when not challenged with pathological stimuli. Since VE-Cadherin inducible Cre-recombination in adult mice has been described to be mosaic-like and partial in LSECs,<sup>50</sup> it is not clear whether angiocrine HGF is required for the physiological maintenance of liver function and embryonic development. Therefore, Stab2-Cre mice<sup>45,51</sup> were used to generate a cell-type-specific HGF-KO in LSECs (HGF<sup>ΔLSEC</sup>) that is active from E9.5 onwards and thereby allows the comprehensive analysis of angiocrine HGF during liver development, physiological homeostasis, and regeneration.

The aims of this study are summarised as follows:

- Investigate the organismal growth and liver development of the LESC-specific HGF KO mice.
- Determine the role of hepatic angiocrine HGF signalling in liver regeneration induced by partial hepatectomy in mice.
- Analyse the HGF/c-Met signalling pathway during liver regeneration.
- Elucidate the mechanisms of hepatic angiocrine HGF signalling during liver regeneration.

# 3 Materials and methods

## 3.1 Materials

### 3.1.1 Chemicals and reagents

<b>Chemicals and reagents</b>	<b>Supplier</b>
2-Mercaptoethanol	Sigma-Aldrich, USA
6×DNA Loading Dye	Thermo Fisher Scientific, USA
Acrylamide Solution	Carl ROTH, Germany
Agarose	Carl ROTH, Germany
Albumin Fraction V (BSA)	Carl ROTH, Germany
Ammonium Persulfate (APS)	Sigma-Aldrich, USA
Citric Acid	Carl ROTH, Germany
DAB+Chromogen System	Dako, Agilent Technologies, USA, Agilent technologies, USA
DirectPCR Lysis Reagent Tail	PEQLAB, VWR, Germany
DNA Ladder	Thermo Fisher Scientific, USA
ECL detection reagent	Amersham, GE Healthdcare, USA
Ethanol	Carl ROTH, Germany
Glycine	Carl ROTH, Germany
Hematoxylin	Merck, Germany
Histowax	Leica, Germany
Hydrogen Peroxide (30%)	Carl ROTH, Germany
Isoflurane	CP-Pharma, Germany

Isopropanol	Carl ROTH, Germany
LDS sample buffer (4x)	Thermo Fischer Scientific
Methanol	Merck, Germany
Milk Powder Blotting Grade	Carl ROTH, Germany
MOPS	Carl ROTH, Germany
Mounting Medium	Dako, Agilent Technologies, USA
Nitrocellulose Membranes	Bio-Rad, USA
NuPAGE LDS Sample Buffer (4x)	Thermo Fisher Scientific, USA
NuPAGE Sample Reducing Agent (10x)	Thermo Fisher Scientific, USA
PageRuler Prestained Protein Ladder	Thermo Fisher Scientific, USA
Paraformaldehyde (PFA)	Apotheke TU München, Germany
Phosphatase inhibitor cocktail	Roche diagnostics, Switzerland
Phosphate Buffered Saline (PBS) pH7.4	Sigma-Aldrich, USA
Protease inhibitor cocktail	Roche diagnostics, Switzerland
PBS powder without Ca <sup>2+</sup> , Mg <sup>2+</sup>	Biochrom AG, Germany
Proteinase K	Carl ROTH, Germany
RIPA Buffer	Cell Signaling Technology
RNA free water	Thermo Fisher Scientific, USA
Roticlear	Carl ROTH, Germany
Rotiphorese Gel 30 (37,5:1)	Carl ROTH, Germany

Sample reducing buffer (10x)	Thermo Fisher Scientific, USA
SDS Ultra Pure	Carl ROTH, Germany
Sodium Chloride	Merck, Germany
Sodium Citrate	Merck, Germany
Sodium Hydroxide	Carl ROTH, Germany
Sodium Phosphate	Merck, Germany
TEMED	Carl ROTH, Germany
Tris Base	Merck, Germany
Tween 20	Carl ROTH, Germany

### 3.1.2 Antibodies

<b>Primary antibodies</b>	<b>Supplier</b>
Mouse anti-BrdU monoclonal antibody (#5292)	Cell Signaling Technology, Germany
mouse anti-Ki67 antibody (#550609)	BD Biosciences, USA
rabbit anti-phospho c-Met (Tyr1234/1235) (#3077)	Cell Signaling Technology, Germany
mouse anti-c-Met (#3127)	Cell Signaling Technology, Germany
mouse anti-HGF (NBP1-19182)	Novus Biologicals, USA
mouse anti-GAPDH(sc-32233)	Santa Cruz, USA
mouse anti- $\beta$ -actin (sc-69879)	Santa Cruz, USA
mouse anti-Deptor (A-3) (sc-398169)	Santa Cruz, USA
<b>Secondary antibodies</b>	<b>Supplier</b>

EnVision-System- Labelled Ploymer anti-mouse (K4001)	HRP	Dako, Agilent Technologies, USA
EnVision-System- Labelled Ploymer anti-rabbit (K4011)	HRP	Agilent Technologies, USA
Anti-Rabbit IgG HRP Conjugate (W401B)		Promega, USA
Anti-Mouse IgG HRP Conjugate (W402B)		Promega, USA

### 3.1.3 Laboratory equipments

<b>Equipment name</b>	<b>Supplier</b>
Analytic balance	METTLER, Germany
Balance	SCALTEC, Germany
Biophototer	Eppendorf, Germany
Centrifuge	Eppendorf, Germany
Electrophoresis / Electroblotting equipment / power supply	Thermo Fisher Scientific, USA
Freezer -20 °C	LIEBHERR, Switzerland
Freezer -80 °C	Heraeus, Germany
gel electrophoresis	BioRad, USA
Microplate Reader	Thermo Fisher Scientific, USA
Microplate washer (HydroFlex)	TECAN, Switzerland
Microscope	Leica, Germany
Microwave oven	SIEMENS, Germany
Multi Detection System (GloMax)	Promega, USA
Nanodrop	Thermo Fisher Scientific, USA

PH-meter	Thermo Fisher Scientific, USA
Real-time PCR amplification and detection instrument (Lightcycler 480)	Roche, Switzerland
Refrigerator 4 °C	COMFORT, Switzerland
Roller mixer	STUART, UK
Scanner	Canon, Japan
Sterilgard Hood	Thermo Fisher Scientific, USA
Surgical microscope (Zeiss Stemi DV4 SPOT)	Zeiss, Germany
Tissue embedding machine	Leica, Germany
Tissue processor	Leica, Germany
Trans-Blot SD Wet Transfer Cell	BioRad, USA
Vortex Mixer	NEOLAB, Germany

### 3.1.4 Kits

<b>Name of Kits</b>	<b>Supplier</b>
BCA Protein Assay Kit (REF 23225)	Thermo Fisher Scientific, USA
KAPA SYBR FAST Kit (KK4611)	Sigma-Aldrich, USA
NucleoSpin RNA Kit (740955.250)	MACHEREY-NAGEL, Germany
QuantiTect Reverse Transcription Kit (Cat. no. 205313)	QIAGEN, Germany
RNeasy Mini Kit (REF 74134)	QIAGEN, Germany

### 3.1.5 Buffers and solutions

- **Western blotting buffer**

#### 10x Tris Buffered Saline (TBS)

Tris base	12.1 g
NaCl	85 g
Distilled Water	800 ml
Adjust pH to 7.4 with	5 M HCl
Constant volume with distilled water to	1000 ml

#### Electrophoresis buffer

MOPS	209.2 g
Tris Base	121.2 g
SDS	20 g
EDTA-free acid	6 g
Constant volume with distilled water	1000 ml

#### Transfer Buffer

Tris base	29.1 g
Glycine	14.7 g
Methanol	1000 ml
SDS	0.1875 g
Constant volume with distilled water	to 5 L

Washing buffer (TBST)

10xTBS	100 ml
Tween 20	0.5 ml
Constant volume with distilled water	to 1000 ml

- **Immunohistochemistry buffers**

20x Citrate buffer

Citric acid (Monohydrate)	21.0 g
Distilled water	300 ml
Adjust to pH 6,0 with	5 M NaOH
Constant volume with distilled water to	to 500 ml

Washing Buffer (1xTBS+0.1%BSA, TBSA)

10xTBS	100 ml
BSA	1 g
Constant volume with distilled water to	1000 ml

## 3.2 Methods

### 3.2.1 Generation of HGF<sup>ΔLSEC</sup> mouse model

HGF loss-of-function in LSECs (Stab2-iCre<sup>tg/wt</sup>;HGF<sup>fl/fl</sup>=HGF<sup>ΔLSEC</sup>) was achieved by crossing Stab2-iCre<sup>tg/wt</sup>;HGF<sup>fl/wt</sup> with HGF<sup>fl/fl</sup> mice.(Phaneuf, Moscioni et al. 2004) The animal experiments were approved by the animal ethics committee (Regierungspraesidium Karlsruhe). All animals were housed under SPF (specific-pathogen-free) conditions in an animal facility (Heidelberg University). The animal experiments were performed in accordance with Federal Animal Regulations and were institutionally approved by the District Government of Upper Bavaria and performed under institutional guidelines (ROB-55.2-2532.Vet\_02-18-64). For this thesis we were allowed to use these generated HGF<sup>ΔLSEC</sup> mice for our experiments.

### 3.2.2 Partial hepatectomy

Seventy percent PH was performed by removal of the left lateral lobe and the median lobe, following published methods.(Mitchell and Willenbring 2008) The operations were performed under general anaesthesia with inhaled isoflurane between 8:00 to 12:00 in the morning. Male mice at the age of 8–12 weeks kept on a 12 h day/night cycle with free access to food and water were used in all experiments. After PH, all experimental mice were regularly examined to recognize pain, distress, and discomfort. The following parameters were applied: No reaction or aggressiveness or expressions of pain during handling, pain when walking, permanent chewing attitude, self-isolation, abnormal posture, paralysis, wound dehiscence, more than 20 % weight loss. Once the score of a mouse reached the standard of a humane end point, the mouse was euthanised immediately. Mice that remained in the experiment were given intraperitoneal injections of 1 mg Bromodeoxyuridine (BrdU, BD Biosciences, USA) 2 h before sacrifice at different time points (0 h, 12 h, 24 h, 48 h, 72 h, 96 h, or 168 h) after surgery. Necropsy was carried out immediately after euthanasia. The removed liver lobes were immediately weighed, fixed in 4%

paraformaldehyde or flash-frozen in liquid nitrogen, and stored at -80 °C for subsequent genomic and proteomic analyses.

### **3.2.3 Preparation for paraffin-embedded liver sections**

Liver tissue samples were fixed in 4% paraformaldehyde at room temperature (15° to 25°C) for 48–72 h, then transferred into PBS (Phosphate-buffered saline), dehydrated in a graded alcohol series, and embedded in paraffin. The paraffin embedded liver tissues were sectioned to produce 3.5 µm sections.

### **3.2.4 Immunohistochemistry**

Immunohistochemistry was performed using the Dako Envision System (Dako, Agilent Technologies, USA) following the listed steps.

- Paraffin-embedded tissue sections were deparaffinised with Roticlear three times for 10 min each, rehydrated with a descending alcohol series (100%, 100%, 100%, 96%, 70%, 50%, 2 min each), and then put in dH<sub>2</sub>O for 2 min.
- Antigen retrieval was performed by treating the slides with citrate buffer (pH 6.0) in a 600 °C microwave oven for 15 min. Then, the slides were cooled for 20 min at room temperature (15° to 25°C).
- The slides were washed in TBS/0.1% BSA for 5 min and blocked with 3% peroxidase, which was diluted with absolute methanol, for 10 min in the dark. The slides were then washed again in TBS/0.1% BSA for 5 min three times.
- The reaction was blocked with 10% goat serum for 1 h at room temperature (15° to 25°C).
- The primary antibodies were diluted to the recommended concentrations in PBS, pipetted onto the slides, and incubated overnight at 4 °C in a wet box.
- The slides were rinsed three times with TBS/0.1% BSA and incubated with horseradish peroxidase HRP-conjugated secondary antibody for 1 h at room temperature (15° to 25°C).

- The slides were counterstained with hematoxylin and washed under running tap water for 15 min.
- The slides were washed with TBS/0.1% BSA three times. Then, an enzymatic reaction with substrate solution (0.5 mg DAB/phosphate buffer) was performed on the slides. The reaction was stopped in water when the slide was ready.
- The tissue was dehydrated in an ascending alcohol series (50%, 70%, 96%, 100%, 100%, 100%, 2 min each) and cleared in Roticlear three times, for 10 min each.
- Finally, the slides were mounted with mounting medium.

### **3.2.5 Hematoxylin & eosin (H&E) staining**

- Paraffin-embedded tissue sections (3.5  $\mu\text{m}$  thick) were deparaffinised with Roticlear 3 times for 10 min each and rehydrated with a descending alcohol series (100%, 100%, 100%, 96%, 70%, 50%, 2 min each).
- The slides were stained with a hematoxylin solution and washed under running tap water for 20 min.
- The slides were counterstained with eosin.
- The slides were dehydrated with an ascending alcohol series (50%, 70%, 96%, 100%, 100%, 100%, 2 min each) and cleared in Roticlear three times, for 10 min each.
- Finally, the slides were mounted with mounting medium.

### **3.2.6 Periodic acid-Schiff (PAS) staining**

- Paraffin-embedded tissue slides were deparaffinized with Xylene 2 times for 5 minutes each and rehydrated with a descending alcohol row (100%, 96%, 70%) 2 times for 2 minutes each, and then in dH<sub>2</sub>O 1 minute for 2 times.
- The slides were stained in periodic acid for 5 minutes, and then in dH<sub>2</sub>O 1 minute for 2 times.
- The slides were counterstained in Schiff's reagent for 15 minutes.

- The slides were washed in running tap water for 5 minutes, and then in dH<sub>2</sub>O 1 minute for 2 times.
- The slides were dehydrated in ascending alcohol rows (70%, 96%, 100%) 2 times for 2 minutes each, and then in Xylene 2 times for 2 minutes.
- Finally, the slides were mounted with mounting medium.

### **3.2.7 Image processing**

Sections were photographed with an Axio microscope (Zeiss, Germany). Images processing was performed using ImageJ software (NIH, USA). The percentage of proliferative hepatocytes was determined by examination of at least five random 200× fields in more than five different sections.

### **3.2.8 RNA isolation from liver tissue**

Total RNA was extracted from mouse liver tissue using an RNeasy Mini Kit (REF 74134) (Qiagen, Germany) and NucleoSpin RNA Kit (740955.250) (MACHEREY-NAGEL, Germany) according to the manufacturer's instructions.

RNeasy Mini Kit (Qiagen) protocol:

- Approximately 30 mg of mouse liver tissue was placed in 400 µL RLT with 0.4 µL β-ME (2-Mercaptoethanol). The lysate was homogenised for 5 min and then centrifuged for 3 min at maximum speed. The supernatant (350 µL) was collected.
- 350 µL of 70% ethanol was added to the lysate and mixed by pipetting.
- 700 µL of the sample was transferred to an RNeasy Mini spin column placed in a 2 mL collection tube and centrifuged for 15 s at 8000 × *g*. The flow-through was discarded.
- A volume of 700 µL Buffer RW1 was added to the RNeasy Mini spin column. The columns were centrifuged for 15 s at 8000 × *g* and the flow-through was discarded.
- Buffer RPE (500 µL) was added to the RNeasy spin column and centrifuged for 15 s at 8000 × *g*. The flow-through was discarded.

- Buffer RPE (500  $\mu$ L) was added to the RNeasy spin column and centrifuged for 2 min at 8000  $\times g$ . The RNeasy spin columns were placed into new 2 mL collection tubes and centrifuged at full speed for 1 min to further dry the membrane.
- The RNeasy spin columns were placed into new 1.5 mL collection tubes. A volume of 30  $\mu$ L RNase-free water was added directly to the spin column membrane and the columns were centrifuged for 1 min at 8000  $\times g$  to elute the RNA.

NucleoSpin RNA Kit (MACHEREY-NAGEL, Germany) protocol:

- A total of 30 mg of liver tissue was homogenised.
- A NucleoSpin filter was placed in a 2 mL collection tube and the homogenate was added and centrifuged for 1 min at 11,000  $\times g$  to filter the lysate.
- The NucleoSpin filter was discarded and 350  $\mu$ L ethanol (70 %) was added to the homogenised lysate and mixed by pipetting up and down (five times).
- Bind RNA. For each preparation, one NucleoSpin RNA column was placed into a collection tube. The lysate was pipetted up and down 2–3 times and loaded onto the column to bind the RNA. The columns were centrifuged for 30 s at 11,000  $\times g$  and then placed into new collection tubes.
- The silica membranes were desalted by adding 350  $\mu$ L MDB and centrifuging at 11,000  $\times g$  for 1 min to dry the membrane.
- To digest the DNA, the DNase reaction mixture was prepared in a sterile 1.5 mL microcentrifuge tube: For each isolation, 10  $\mu$ L reconstituted rDNase was added to 90  $\mu$ L rDNase Reaction Buffer. The tubes were mixed by flicking. A volume of 95  $\mu$ L DNase reaction mixture was applied directly onto the centre of the silica membrane of each column and incubated at room temperature (15° to 25°C) for 15 min.
- The RNA was washed by adding 200  $\mu$ L Buffer RAW2 to the NucleoSpin RNA columns and centrifuging for 30 s at 11,000  $\times g$ . The columns were placed into new 2 mL collection tubes.

- The RNA was washed a second time by adding 600  $\mu\text{L}$  Buffer RA3 to the NucleoSpin RNA columns and centrifuging for 30 s at  $11,000 \times g$ . The flow-through was discarded and the columns were placed back into the collection tubes.
- The RNA was washed a third time by adding 250  $\mu\text{L}$  Buffer RA3 to the NucleoSpin RNA columns and centrifuging for 2 min at  $11,000 \times g$  to dry the membrane completely. The columns were placed into nuclease-free collection tubes.
- The RNA was eluted in 60  $\mu\text{L}$  RNase-free H<sub>2</sub>O, and centrifuged at  $11,000 \times g$  for 1 min.

The RNA concentrations were determined using a NanoDrop (Thermo Fisher Scientific, USA ). The RNA samples were stored at  $-80\text{ }^{\circ}\text{C}$  before use.

### 3.2.9 Complementary DNA reverse transcription

Complementary DNA (cDNA) was synthesised using a QuantiTect Reverse Transcription Kit (Cat. no. 205313) (QIAGEN).

Component	Volume
Template RNA	Variable (1 $\mu\text{g}$ )
RNase-free water	Variable
gDNA wipeout buffer	2 $\mu\text{l}$

- The RNA template was thawed on ice.
- The genomic DNA elimination reaction was prepared on ice, incubated for 2 min at  $42\text{ }^{\circ}\text{C}$ , then returned immediately to ice.
- The reverse-transcription master mix was prepared on ice.

<b>Component</b>	<b>Volume</b>
Quantiscript Reverse Transcriptase	1 µl
Quantiscript RT Buffer	4 µl
RT Primer Mix	1 µl
Entire genomic DNA elimination reaction	14 µl
<b>Total volume</b>	<b>20 µl</b>

- Template RNA (14 µL) was added to each tube containing reverse-transcription master mix and incubated for 15 min at 42 °C.
- The reactions were incubated for 3 min at 95 °C to inactivate the Quantiscript Reverse Transcriptase.
- The reverse-transcription reactions were placed on ice and used for real-time PCR or stored at -20 °C.

### 3.2.10 Quantitative reverse-transcription PCR (qRT-PCR)

Primers were designed using Primer-BLAST (<http://www.ncbi.nlm.nih.gov/tools/primer-blast/>) and PrimerBank (<https://pga.mgh.harvard.edu/primerbank/>). qRT-PCR was performed in a LightCycler 480 real-time PCR machine (Roche, Switzerland) using a KAPA SYBR FAST Kit (KK4611; Sigma-Aldrich, USA). The relative mRNA expression levels were quantified normalising against GAPDH.

#### qRT-PCR primer sequences

<b>Primer name</b>	<b>Primer sequence(5' &gt; 3')</b>
HGF forward	GGTTTGGCCATGAATTTGACCT
HGF reverse	GGCAAAAAGCTGTGTTTCATGGG
GAPDH forward	AGGTCGGTGTGAACGGATTTG
GAPDH reverse	TGTAGACCATGTAGTTGAGGTCA

### qRT-PCR reaction component

Component	Volume
SYBR Green SuperMix	12.5 $\mu$ l
Primers	2 $\mu$ l
cDNA template	5 $\mu$ l
ddH <sub>2</sub> O	3 $\mu$ l
Total	25 $\mu$ l

### qRT-PCR cycling protocol

Temperature	Time
1. 95 °C	5 min
2. 95 °C	10 seconds
3. 60 °C	10 seconds
4. 72 °C	10 seconds
5. 45 cycles for steps 2-4	
6. Melt-curve analysis: 95°C 5 seconds hold, 65°C 1min hold, 97°C	
7. 40°C	30 seconds

### 3.2.11 DNA isolation from mouse tails

- A 0.3 cm piece of mouse tail and DirectPCR Lysis Reagent (Tail) was used for DNA isolation.
- A volume of 80  $\mu$ L DirectPCR Tail containing 8  $\mu$ L freshly prepared Proteinase K was added to a 0.3 cm piece of mouse tail.
- The tube was rotated in a rotating hybridisation oven at 55 °C overnight.
- The crude lysates were incubated at 85 °C for 60 min to achieve complete heat inactivation of Proteinase K.
- The samples were centrifuged at maximum speed for 2 min and the supernatants were collected.

### 3.2.12 Genotyping

The genotype of the mice was determined by PCR with specific pairs of primers according the following protocols.

#### Genotype reaction mix

Component	Volume
PCR Master Mix, 2x	12.5 $\mu$ l
Sense primer (10 $\mu$ M)	0.5 $\mu$ l
Antisense primer (10 $\mu$ M)	0.5 $\mu$ l
DNA template	1 $\mu$ l
RNase-free water	10.5 $\mu$ l
Total volume	25 $\mu$ l

#### Genotype primer sequences

Primer name	Primer sequence(5' > 3')
iCre forward	AAGAACCTGATGGACATGTTTCAGG
iCre reverse	TCTGTCAGAGTTCTCCATCAGGGA

HGF forward	TGACTACGCTGTTCATTCAAGTGC
HGF reverse	CCATTTCTTCAGAGGCAGATGC

### PCR cycling protocol

Temperature	Time
1. 94 °C	60 seconds
2. 94 °C	30 seconds
3. 58 °C	30 seconds
4. 72 °C	60 seconds
5. 40 cycles for 2-4 steps	
6. 72 °C	10 minutes
7. 3°C	continuous

- DNA was run on a 2% agarose gel in 1×TBE at 150 V for 35 min.

#### 3.2.13 Protein extraction from liver tissue

- Liver tissues were lysed from snap frozen liver using 1×RIPA buffer (Cell Signaling Technology, Germany).
- The 1×RIPA buffer was made by mixing 1 mL 10×RIPA buffer + 9 mL dH<sub>2</sub>O + 1 tablet phosphatase inhibitor cocktail tablet (PhosSTOP Easypack, Roche) + 1 tablet EDTA-free Protease Inhibitor Cocktail (Complete mini, Roche).
- A total of 100 mg frozen liver tissue was put into 300 µL 1×RIPA buffer with a steel bead and disrupted with a homogeniser for 5 min.
- The homogenates were spun at full speed for 20 min at 4 °C to remove cell debris.

- The supernatants were carefully removed and kept at  $-80\text{ }^{\circ}\text{C}$  until use.

### 3.2.14 Protein detection and quantitation

A Micro BCA Protein Assay Kit (Thermo, 23225) was used to determine the concentration of proteins.

- The BCA reagent was freshly prepared by adding 4%  $\text{CuSO}_4$  to the standard solution and protein solution at a ratio of 1:50.
- Then, 5  $\mu\text{L}$  of protein sample or the standard was pipetted into a 96-well plate and mixed with 200  $\mu\text{L}$  of the prepared BCA solution.
- The 96-well plate was placed on a shaker for 30 sec.
- The plate was covered and incubated at  $37\text{ }^{\circ}\text{C}$  for 30 min.
- The plate was cooled to room temperature ( $15^{\circ}$  to  $25^{\circ}\text{C}$ ) and the absorbance was measured at a wavelength of 570 nm.
- Finally, the protein concentration was calculated ( $R^2 > 0.95$ ).

### 3.2.15 Western blotting

- The protein denature mixture was denatured at  $70\text{ }^{\circ}\text{C}$  for 10 min.

#### Protein denature mix

Component	Volume
Protein	Variable (20 $\mu\text{g}$ )
Water	14 $\mu\text{l}$ -volume of protein
NuPAGE LDS Sample Buffer 4x	5 $\mu\text{l}$
NuPAGE Reducing Agent 10x	2 $\mu\text{l}$
Total volume	20 $\mu\text{l}$

- A discontinuous gel system, which involved stacking (5%) and separating gel (7.5–12.5%) layers that differed in their salt and acrylamide concentrations, was used. The gels contained: 30% acrylamide, Tris-HCl 1.5 M pH8.8, Tris-HCl pH6.8, 10% APS, 10% SDS, TEMED (Tetramethylethylenediamine). The

gel percentage selected depended on size of the target protein. Equal amounts of 20 µg protein were loaded into each well of the SDS-PAGE gel, in addition to molecular weight markers (PageRuler Prestained Protein Ladder, 26616, 26625 Thermo Fisher). The proteins were separated by gel electrophoresis (BioRad, USA) in running buffer (25 mM Tris, 192 mM glycine, 0.1% SDS, pH 8.3) at 50 V for 30 min, and then the voltage was increased to 120 V to finish.

- The protein was transferred from the gel to the nitrocellulose membranes (GE Healthcare Life Science, Amersham, UK) ensuring that no air bubbles were trapped in the transfer sandwich. The cassette was put in the transfer tank and placed on ice blocks to prevent overheating. The proteins were transferred onto a nitrocellulose membrane using a Trans-Blot SD Wet Transfer Cell (Bio-Rad, USA). Transfer occurred over 1–2 h at 300 mA.
- Afterwards, the membrane was blocked with 5% non-fat milk for 1 h at room temperature (15° to 25°C) and then incubated with the primary antibody at 4 °C overnight.
- On the second day, the membrane was washed with TBST three times for 10 min and incubated at room temperature (15° to 25°C) in the secondary antibody (Anti-Mouse IgG HRP Conjugate, W402B, Promega, USA; Anti-Rabbit IgG HRP Conjugate, W401B, Promega, USA). The membrane was washed with TBST three times for 10 min.
- ECL Western Blotting Detection reagents (GE Healthcare, Amersham, UK) and SuperSignal West Femto Substrate (Thermo Fisher Scientific) were used for signal development. An image was acquired using darkroom development techniques. The relative protein expression levels were analysed using ImageJ image analysis software.

### **3.2.16 ELISA**

Plasma was collected from male HGF<sup>ALSEC</sup> and control mice when the mice were sacrificed at different time points from 8 to 12 weeks of age.

Serum alanine aminotransferase (ALT) activity in PH mice was detected using an ELISA Kit for Alanine Aminotransferase (SEA207Mu) (Cloud-Clone Corp, USA), according to manufacturer's instructions as follows.

- Wells were prepared for the diluted standard (7 wells), blank (1 well), and sample.
- A volume of 100  $\mu$ L of each dilution of standard, blank, and sample was added into the appropriate wells. The plate was covered with the plate sealer and incubated for 1 h at 37 °C. The liquid was removed from each well but the wells were not washed.
- Then, 100  $\mu$ L of Detection Reagent A working solution was added to each well, the wells were covered with the plate sealer, and the plate was incubated for 1 h at 37 °C.
- The solution was removed and the wells were washed with 350  $\mu$ L of 1 $\times$  Wash Solution using an microplate washer (TECAN, Switzerland) three times.
- Then, 100  $\mu$ L of Detection Reagent B working solution was added to each well, the wells were covered with the plate sealer, and the plate was incubated for 30 min at 37 °C.
- The wash process conducted in step 4 was repeated a total of five times.
- A volume of 90  $\mu$ L of Substrate Solution was added to each well. The wells were covered with a new plate sealer, protected from light, and incubated for 20 min at 37 °C.
- Then, 50  $\mu$ L of Stop Solution was added to each well and mixed by tapping the side of the plate.
- Any drops of water or fingerprints on the bottom of the plate were removed and the surface of the liquid was checked to ensure there were no bubbles. The plates were loaded onto the microplate reader (Thermo Fisher Scientific, USA) and measured at 450 nm immediately.

### **3.2.17 RNA sequencing**

Raw count matrices were imported into R and a differential gene expression analysis was conducted using DESeq2. Dispersion estimates were calculated

setting the option fitType to parametric using all samples available. A Wald test was conducted to detect differences between genotypes for all available time points. A gene was called significantly regulated if the p-value was below 0.05. Genes regulated at the time point 48 h are shown as a heatmap together with the samples collected at the 0 h time point.

### **3.3 Statistics**

All statistics were performed using GraphPad Prism 7.0 (GraphPad, San Diego, California, USA). All data are presented as means  $\pm$  standard error of the mean. Statistical differences were analysed using the two-tailed unpaired Student's t-test, the Mann-Whitney U test, and Chi-square test. Statistical significance was set at  $p < 0.05$ .

## 4 Results

### 4.1 HGF ablation in LSECs results in reduced organismal growth but normal liver development

To analyse the role of LSEC-derived HGF in liver regeneration, homozygous  $HGF^{ex.5\ flox}$  ( $HGF^{fl/fl}$ ) (Phaneuf, Moscioni et al. 2004) were crossed to LSEC-specific *Stab2* promoter-driven Cre mice (*Stab2-iCre*). (Koch, Olsavszky et al. 2017) The mice in this study were generated at the University Medical Center and Medical Faculty Mannheim, Heidelberg University.  $Stab2-iCre^{tg/wt};HGF^{fl/fl}$  ( $HGF^{\Delta LSEC}$ ) mice have a specific deletion of HGF in LSECs but no other hepatic cells.  $Stab2-iCre^{wt/wt};HGF^{fl/fl}$  or  $Stab2-iCre^{wt/wt};HGF^{fl/wt}$  mice were used as control mice.  $HGF^{\Delta LSEC}$  embryos did not reveal any developmental defects (Geraud, Koch et al. 2017) and survived to late adulthood (Figure 5).



Control  $HGF^{\Delta LSEC}$

**Figure 5.** Pictures of control and  $HGF^{\Delta LSEC}$  mice. The control mouse on the left and  $HGF^{\Delta LSEC}$  mice on the right.

Despite no apparent macroscopic differences, HGF<sup>ΔLSEC</sup> mice had lower body weights than the control mice (Figure 6A and 6B). Female HGF<sup>ΔLSEC</sup> mice had lower liver weights, however, the liver-to-body ratio was unaltered in both sexes (Figure 6A and 6B). Furthermore, since the spleen is known to contain Stab2<sup>+</sup> sinusoidal endothelial cells (Geraud, Koch et al. 2017), and endogenous splenic HGF mRNA shows high expression, (Bell, Jiang et al. 1998) the spleen-to-body ratios of HGF<sup>ΔLSEC</sup> mice were analysed and found to be similar to those of the controls, with only female HGF<sup>ΔLSEC</sup> mice having lower spleen weights (Figure 6B).

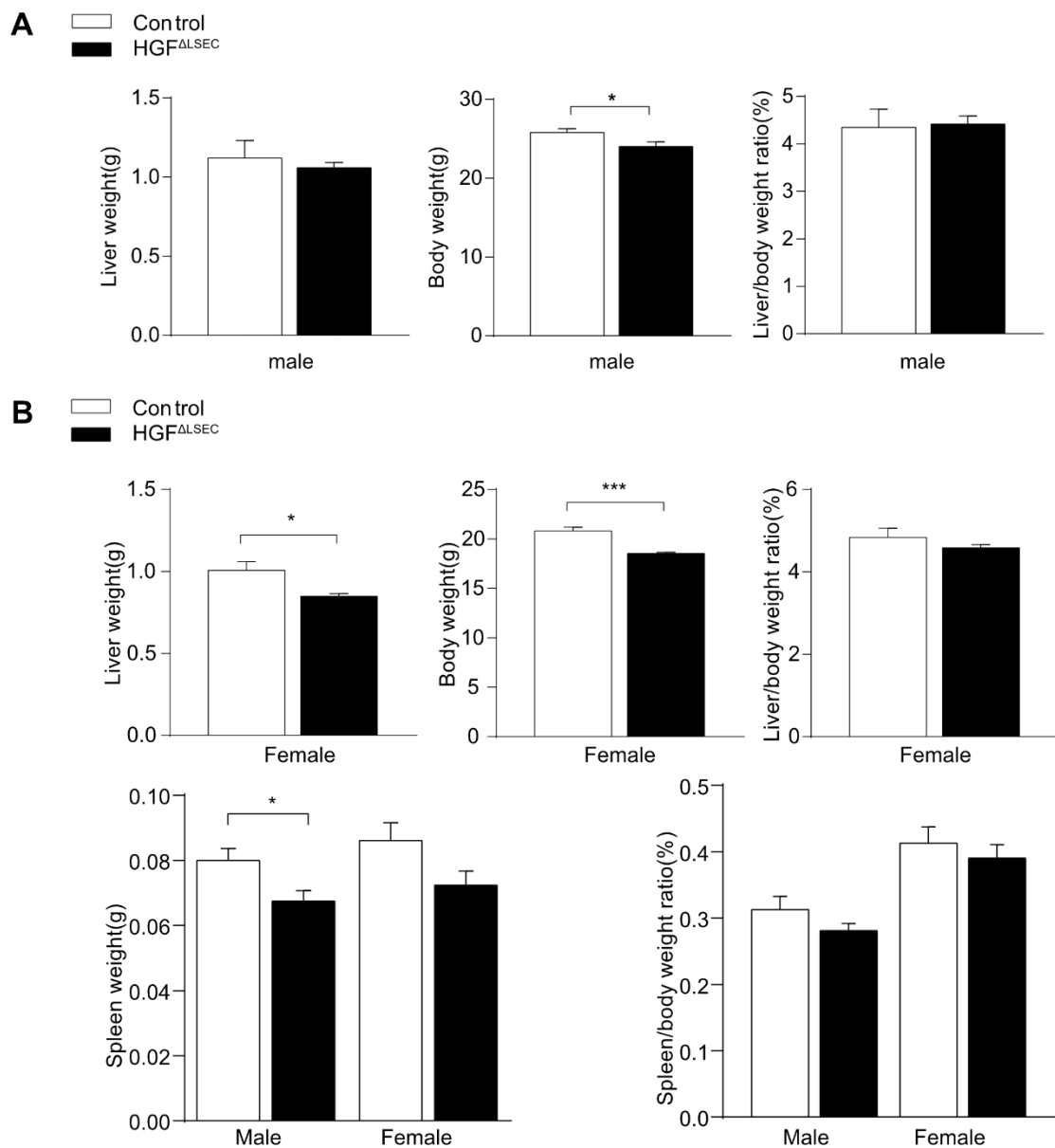


**Figure 6.** Total body weight, liver weight, liver-to-body weight ratio, spleen weight and spleen-to-body weight of the mice. **A.** Total body weight, liver weight, and liver-to-body weight ratio of 9 week old control and HGF<sup>ΔSEC</sup> mice (male, n ≥ 5). The results are represented as mean ± S.E.M. \*p < 0.05. **B.** Total body weight, liver weight, liver-to-body weight ratio of 9 week old control and HGF<sup>ΔSEC</sup> mice (female, n ≥ 5). Spleen weight and spleen-to-body weight ratio of 9 week old control and HGF<sup>ΔSEC</sup> mice (male and female, n ≥ 5). Results are represented as mean ± S.E.M. \*p < 0.05.

Routine histology (H&E, PAS, and Sirius Red) of HGF<sup>ΔSEC</sup> mice did not reveal significant morphological changes, inflammation, or depositions of polysaccharides or collagens compared to control mice (Figure 7). Therefore, except for being slightly but significantly lighter, HGF<sup>ΔSEC</sup> did not show major alterations in liver development or function or any general impairment.

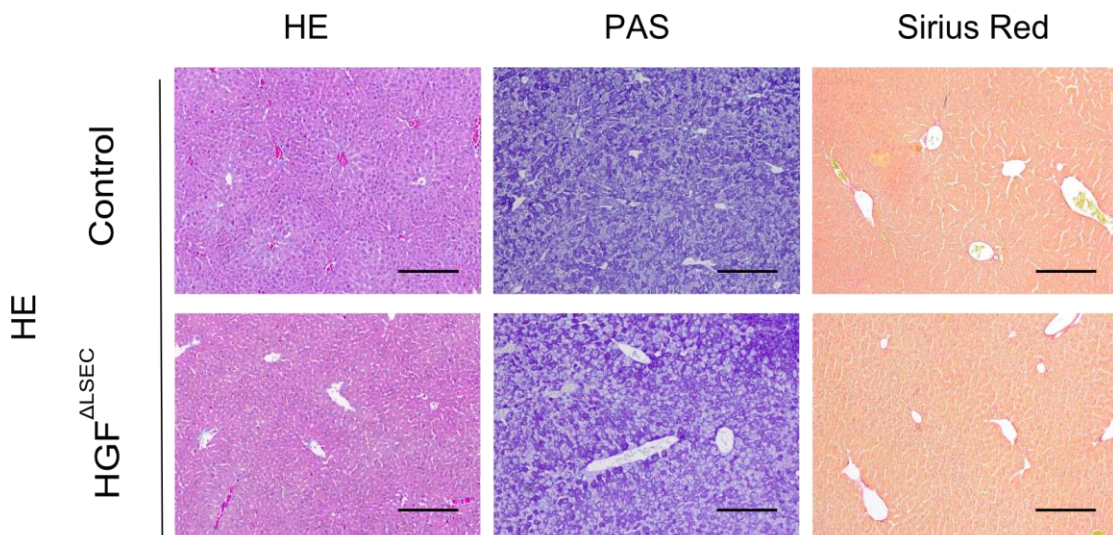


**Figure 7.** H&E, PAS, and Sirius Red staining of liver from HGF<sup>ΔSEC</sup> mice compared to controls (male). Scale bar 100 μm.

## 4.2 Liver regeneration is compromised in HGF<sup>ΔSEC</sup> mice

To further elucidate the role of angiocrine HGF signalling in liver regeneration, 70% PH was performed in both HGF<sup>ΔSEC</sup> and control mice. The liver-to-body weight ratio of both groups gradually recovered to normal at 168 h after PH. HGF<sup>ΔSEC</sup> mice showed a significantly lower liver-to-body weight ratio than the control group at 72 h after PH (Figure 8).

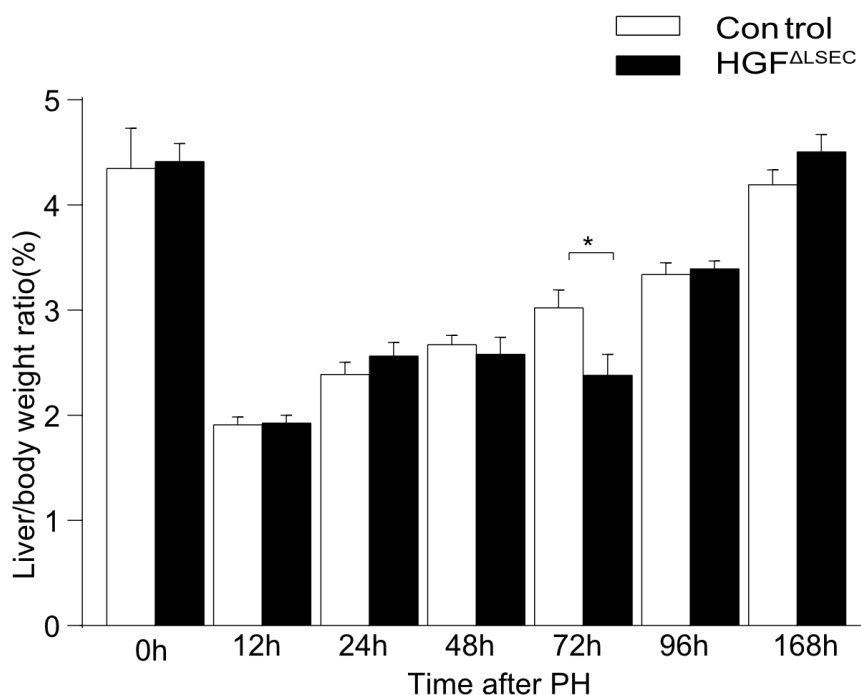


**Figure 8.** Liver-to-body weight ratio of HGF<sup>ΔSEC</sup> and control mice at different time points after 70% PH. Results are represented as mean  $\pm$  S.E.M. \* $p < 0.05$ .

Typically, proliferation of all hepatic cells sharply increase after PH, peaking at 48–72 h post operation. (Miyaoaka, Ebato et al. 2012) Therefore, hepatocytes that entered into the S-phase of the cell cycle were revealed by the incorporation of 5-bromo-2'-deoxyuridine (BrdU). BrdU can be incorporated into the newly synthesised DNA of replicating cells during the S phase of the cell cycle. BrdU staining is used as hepatocyte proliferation marker in our research. Staining for BrdU revealed that hepatocyte proliferation in control mice started at 24 h, reaching a peak at 48 h, and terminating at 168 h after

PH (Figure 9A).

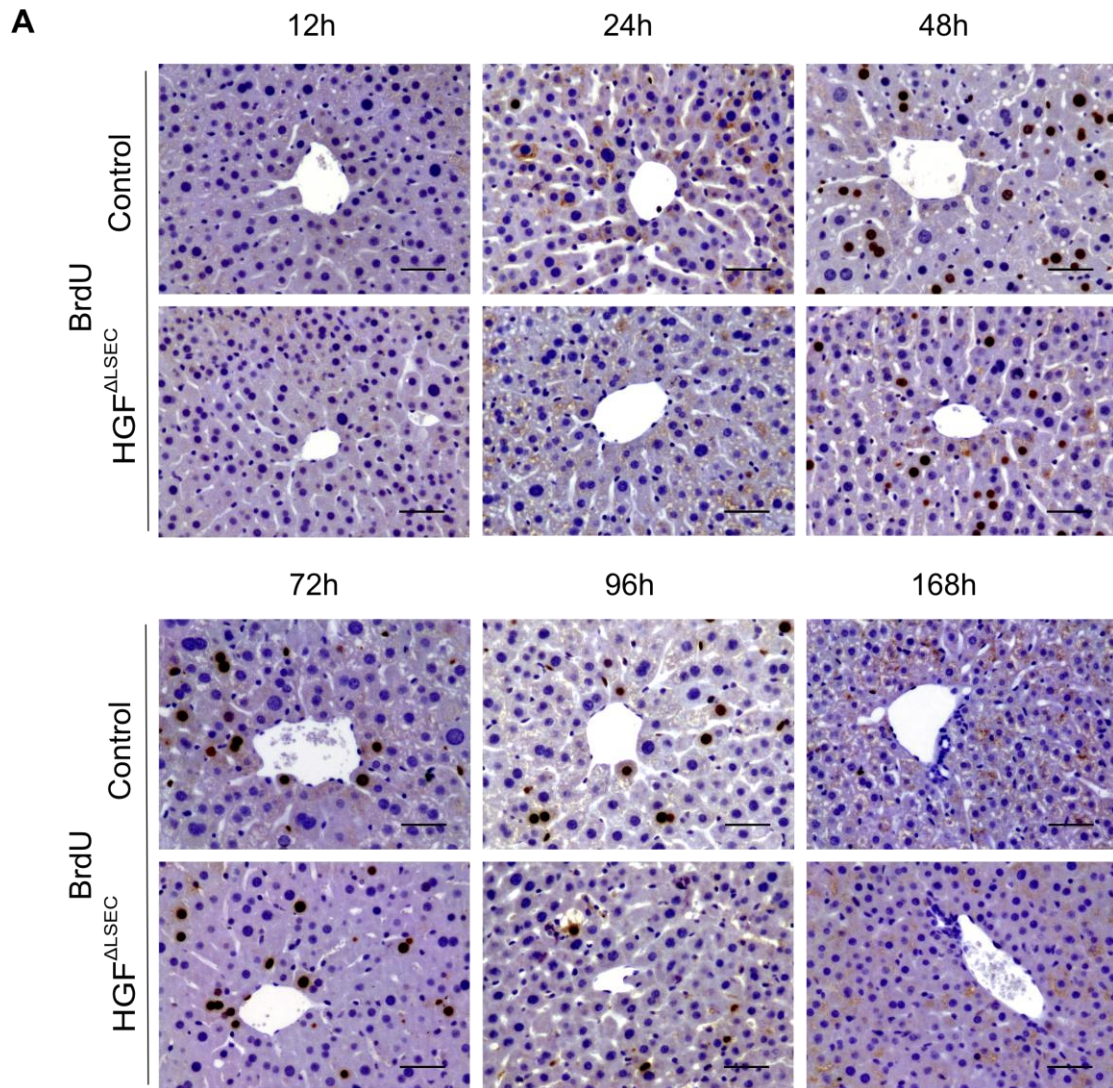


**Figure 9.** BrdU and Ki67 stainings of liver sections. **A.** Representative micrographs of liver sections from HGF<sup>ALSEC</sup> and control mice after 70% PH, immunostained with the BrdU antibody ( $n \geq 5$ ). Scale bar: 200  $\mu$ m.

Ki67 is another widely used marker of proliferating cells. Ki67 protein is present during all active phases of the cell cycle (G1, S, G2, and M), but absent in quiescent cells (G0). (Bruno and Darzynkiewicz 1992) Accordingly, Anti-Ki67 staining of liver sections showed a similar pattern to the BrdU staining (Figure 9B).

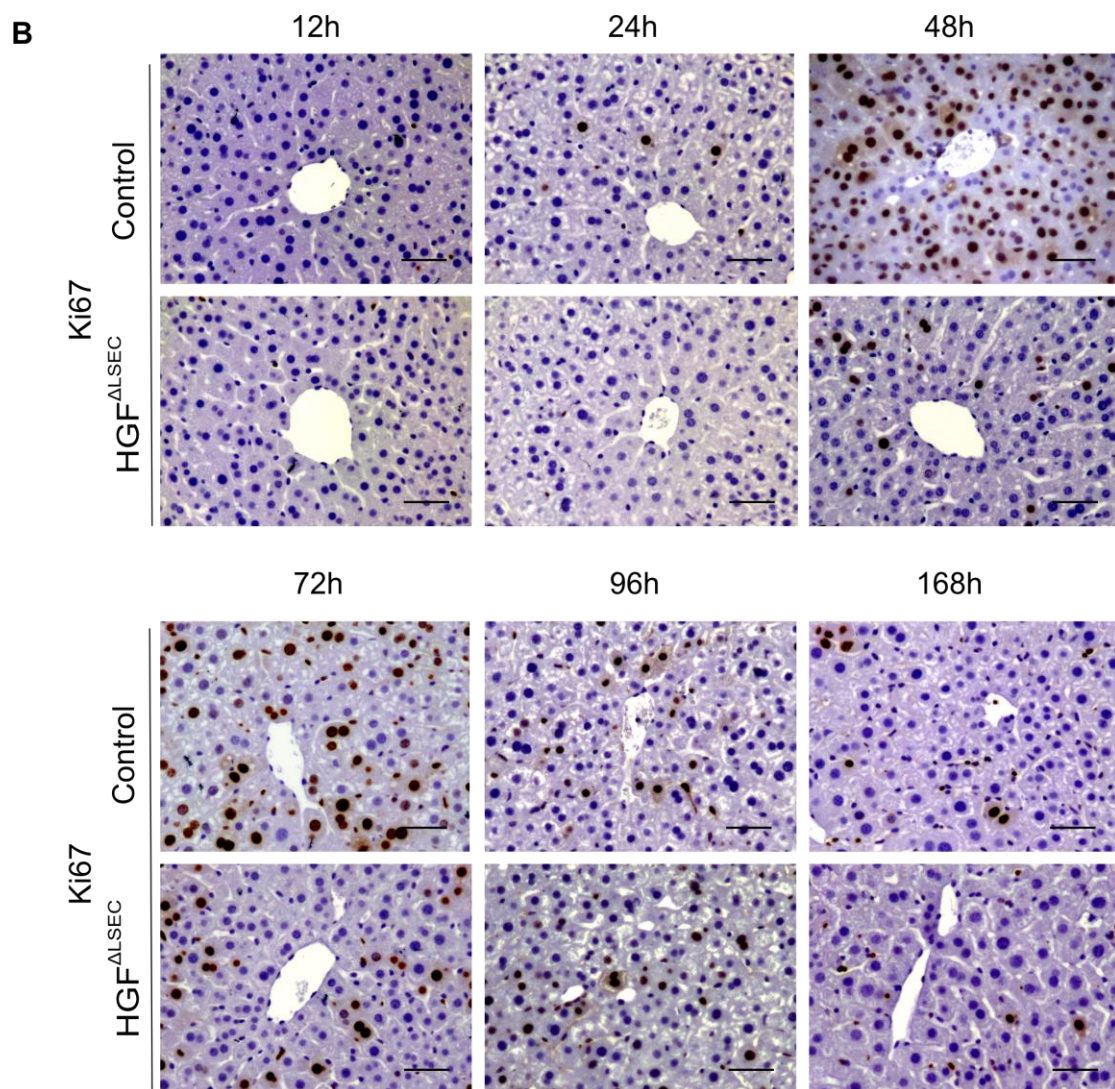


**Figure 9. B.** Representative micrographs of liver sections from HGF<sup>ΔSEC</sup> and control mice after 70% PH, immunostained with Ki67 antibody ( $n \geq 5$ ). Scale bar: 200  $\mu\text{m}$ .

In contrast, the fraction of BrdU-positive hepatocytes in HGF<sup>ΔSEC</sup> mice was significantly lower than control mice at 48 h after PH (Figure 10A). Consistent with this finding, HGF<sup>ΔSEC</sup> mouse livers displayed less Ki67-positive hepatocytes than control mice at this time point (Figure 9B; Figure 10B). These findings indicate that the regenerative capacity of the liver is compromised in

HGF $\Delta$ SEC mice.

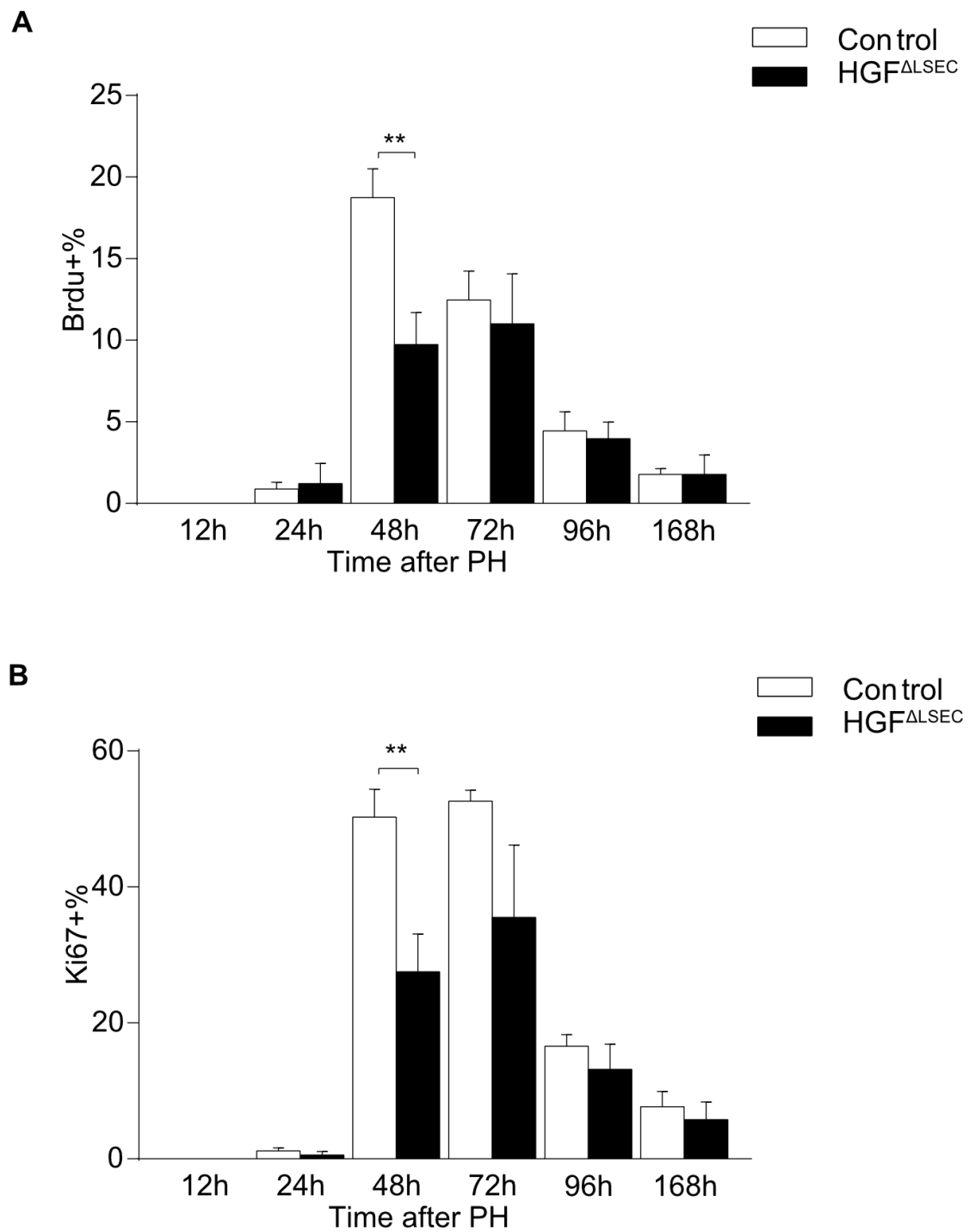


**Figure 10.** Quantification of BrdU and Ki67 positive hepatocytes. **A.** Quantification of BrdU-positive hepatocytes at different time points after 70%

PH. **B.** Quantification of Ki67-positive hepatocytes at different time points after 70% PH. Results are represented as mean  $\pm$  S.E.M. \*\* $p < 0.01$ .

### 4.3 Lethality of HGF <sup>$\Delta$ SEC</sup> mice is higher than control mice after PH

After PH, mice were carefully and regularly observed for signs of pain or distress. As a surrogate for lethality, the number of mice that reached humane endpoints and had to be euthanised was analysed. This only occurred in HGF <sup>$\Delta$ SEC</sup> and not control mice after PH (Table 1). All control mice were healthy and survived up to the designated time points after PH, whereas 12.82% of HGF <sup>$\Delta$ SEC</sup> mice reached the humane endpoint 48–72 h after PH (Table 1). Therefore, HGF <sup>$\Delta$ SEC</sup> mice showed higher lethality than control mice after PH within 168 h.

Mouse lethality after PH within 168h

Genotype	Dead	Total	Lethality (%)
Control	0	34	0
HGF <sup><math>\Delta</math>SEC</sup>	5	39	12.82

**Table 1.** Mouse lethality after partial hepatectomy within 168h. A higher lethality (12.82%) of HGF <sup>$\Delta$ SEC</sup> mice was observed compared to control mice (0%) after PH (Chi-square test,  $p < 0.05$ ).

### 4.4 Liver necrosis in HGF <sup>$\Delta$ SEC</sup> mice is more visible after PH

Assessment of liver histology revealed that a subset of HGF <sup>$\Delta$ SEC</sup> mice had liver necrosis 48–96 h after PH, but no necrotic areas were found in control mice after PH. (Table 2, Figure 11A and 11B)

Mice with liver necrosis after PH (animal numbers)

Time after PH	Control		HGF <sup>ΔLSEC</sup>	
	Necrosis	Normal	Necrosis	Normal
12h	0	5	0	5
24h	0	5	0	5
48h	0	7	3	5
72h	0	5	2	3
96h	0	6	1	5
168h	0	6	0	5

**Table 2.** Numbers of mice with liver necrosis at different time points after partial hepatectomy.

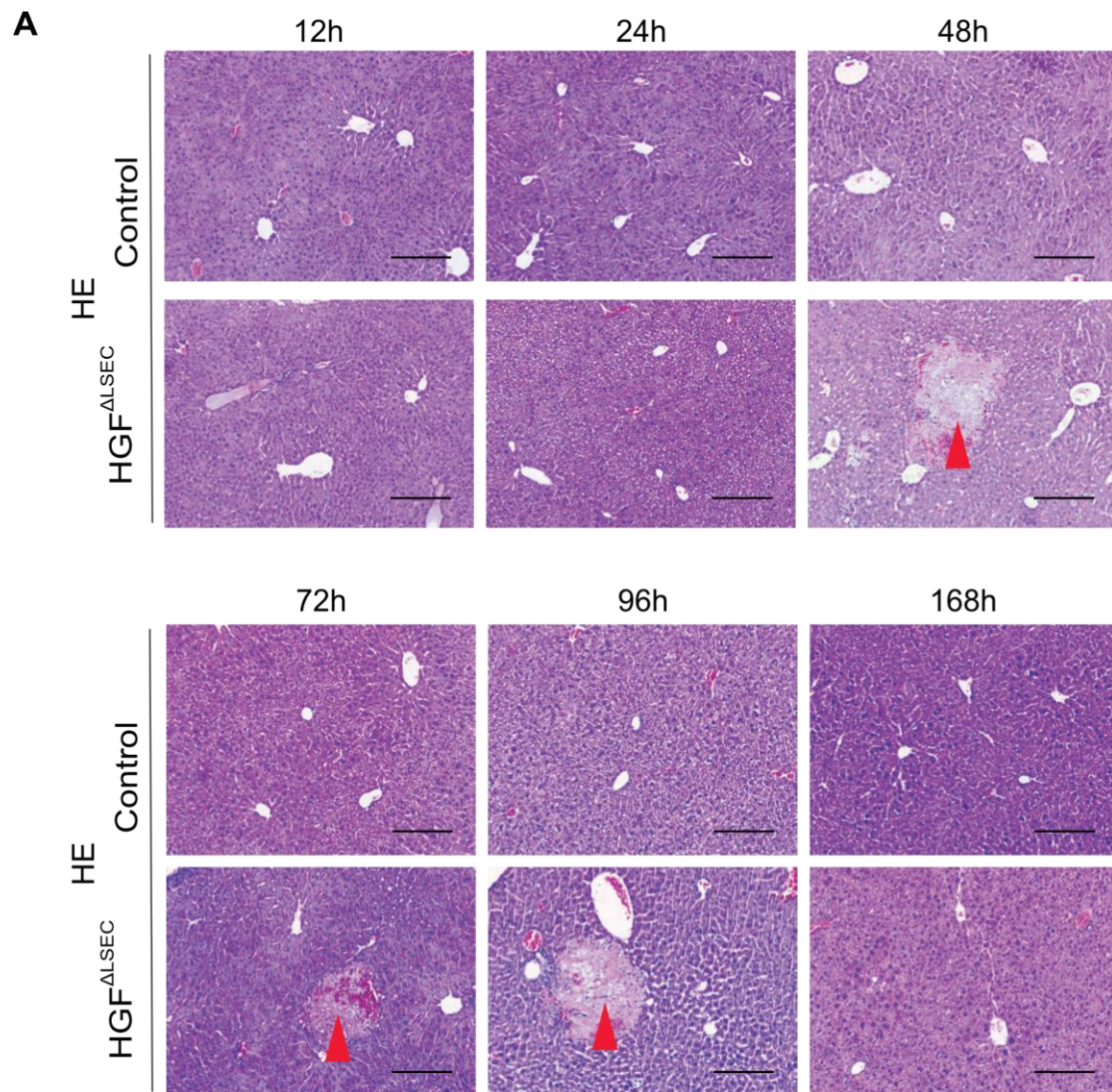


**Figure 11.** H&E staining of liver sections show necrotic areas. **A.** H&E staining of liver sections of HGF<sup>ΔSEC</sup> and control mice at different time points after 70% PH; red triangles indicate necrotic areas of HGF<sup>ΔSEC</sup> mouse livers after 70% PH (n≥5). Scale bar: 100 μm.

**B**

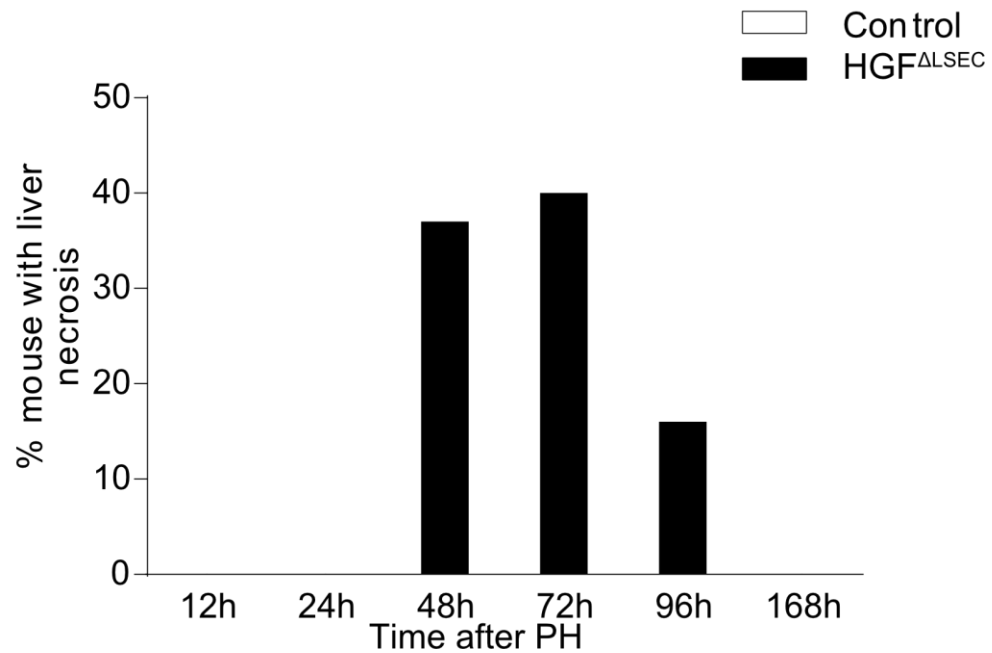


**Figure 11. B.** Percentage of necrotic areas of liver sections from HGF $\Delta$ SEC mice after 70% PH.

#### **4.5 Serum ALT levels of HGF $\Delta$ SEC are elevated after PH**

Serum alanine aminotransferase (ALT) is the most commonly used variable for the assessment of liver injury.(Pratt and Kaplan 2000, Prati, Taioli et al. 2002) It is measured clinically as part of liver function tests.

We determined ALT activity to evaluate liver function after PH. ALT was detected at different time points after PH. ALT values strongly increased after PH in both HGF $\Delta$ SEC and control mice. Higher ALT values were found at 48 and 168 h after PH in HGF $\Delta$ SEC than in control mice (Figure 12).

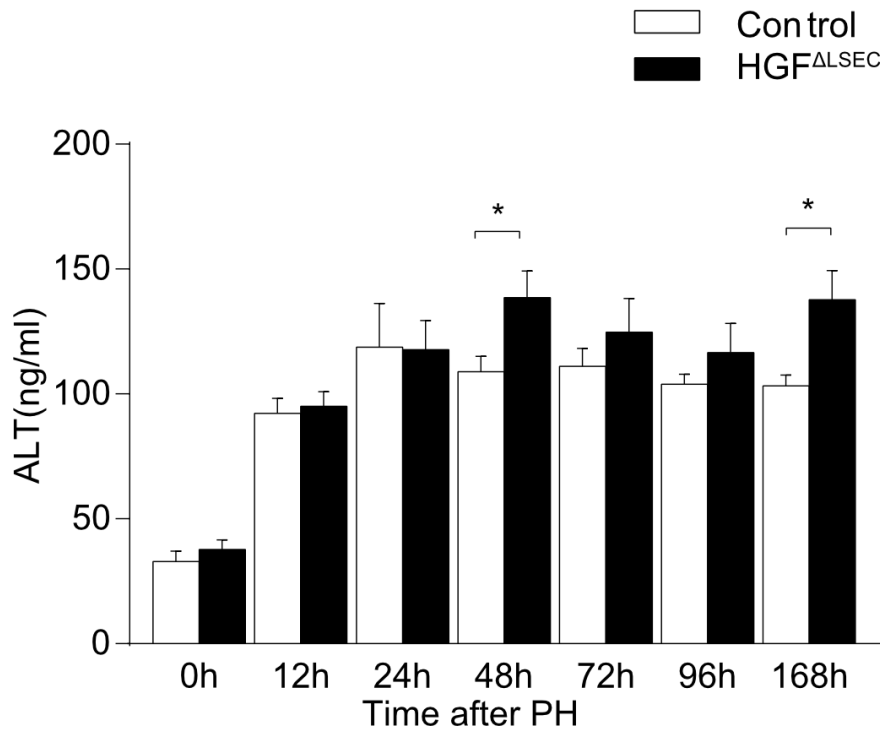


**Figure 12.** ALT activity of serum from HGF $\Delta$ SEC and control mice. ( $n \geq 5$ ). Results are represented as mean  $\pm$  S.E.M. \* $p < 0.05$ .

Overall, the findings of increased lethality, reduced hepatocyte proliferation, and enhanced liver necrosis demonstrate that the regenerative capacity of HGF $\Delta$ SEC mice is indeed impaired after 70% PH.

#### 4.6 HGF mRNA expression of whole liver lysates is downregulated during liver regeneration

Figure 13 shows the kinetics of HGF expression during liver regeneration determined by qRT-PCR analysis of mRNA from whole liver lysates. Evaluation of HGF mRNA expression in the mouse livers at the 0 h time point did not reveal any differences between HGF $\Delta$ SEC mice and control mice. Nevertheless, the relative HGF mRNA expression of HGF $\Delta$ SEC mice at 12 h after PH was significantly decreased than control mice. There are two phases of the liver regeneration process after PH. (Pediaditakis, Lopez-Talavera et al. 2001) The

first phase (the consumptive phase) is from 0–3 h after PH and is characterised by a decline in both single-chain HGF and active two-chain HGF in the total liver homogenates. The second phase (productive phase) is from 3–72 h after PH. It is characterised by an increase in the levels of single-chain HGF and active two-chain HGF. Previous studies have shown that new HGF synthesis is detectable from 3 h and peaks at 12 h after PH.(Pediaditakis, Lopez-Talavera et al. 2001) HGF relative mRNA expression in the liver in our study rose after PH, peaked at 12 h, and gradually returned to normal levels at 96 h. Our results are therefore consistent with previous research.

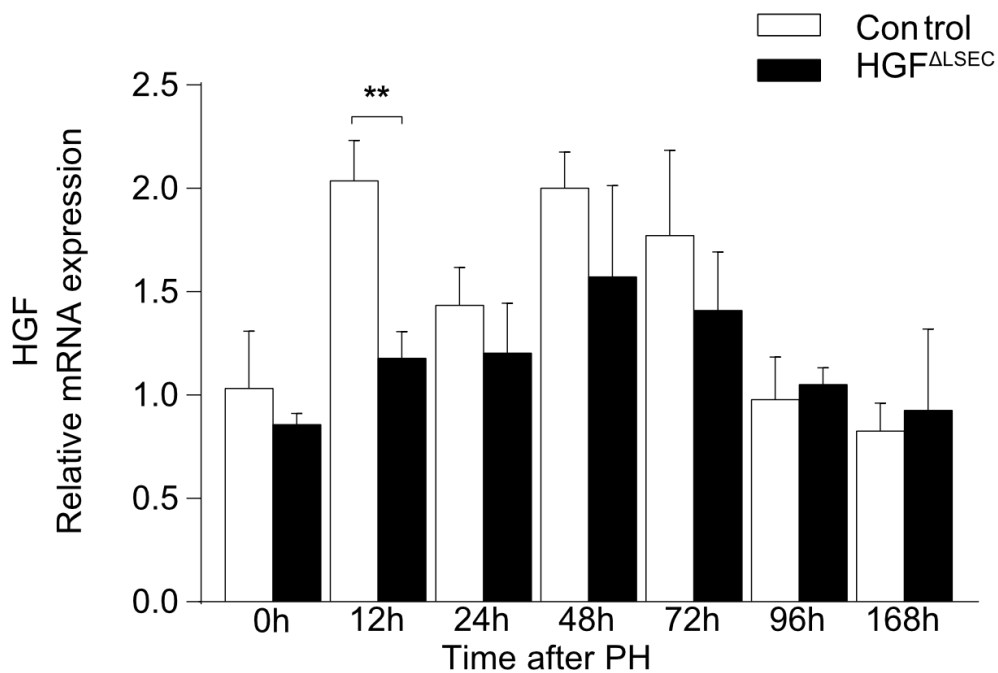


**Figure 13.** qRT-PCR of HGF in livers of HGF<sup>ΔSEC</sup> and control mice at different time points after 70% PH (n=5). GAPDH was used as housekeeping gene. \*\*p < 0.01.

#### 4.7 HGF/c-Met signalling pathway is impaired in HGF<sup>ΔSEC</sup> mice after PH

Previous studies, including work from our group, have shown that the HGF/c-MET signalling pathway provides essential signals for liver regeneration after

PH.(Borowiak, Garratt et al. 2004, Huh, Factor et al. 2004, Ishikawa, Factor et al. 2012, Cheng, Liu et al. 2018) Therefore, the HGF/c-MET signalling pathway was analysed at different time points after PH at the protein level. HGF protein levels significantly increased from 12 h to 72 h after PH in both groups (Figure 14A and 14B). The levels of c-Met phosphorylation showed a similar tendency (Figure 14A). The comparison of HGF<sup>ΔSEC</sup> and control mice revealed a significant decrease in HGF protein levels at 48 h and 72 h after PH in HGF<sup>ΔSEC</sup> mice (Figure 14A). In addition, phosphorylation of c-Met was reduced at the 48 h time point in HGF<sup>ΔSEC</sup> mice (Figure 14B). These results indicate that the HGF/c-Met signalling pathway is impaired in HGF<sup>ΔSEC</sup> mice after PH.

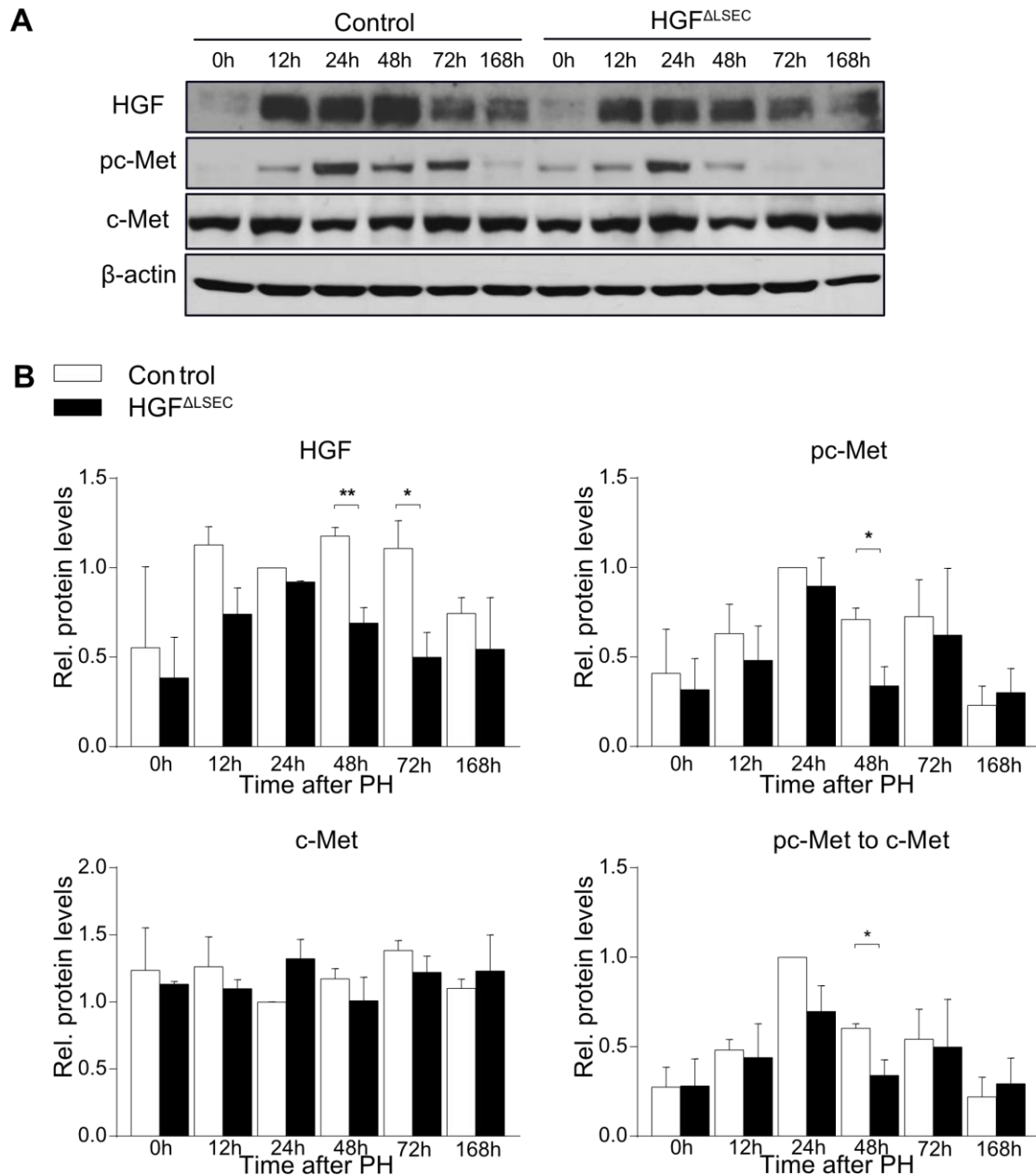


**Figure 14.** Hepatic expression of the HGF/c-Met signalling pathway after 70% PH. **A.** Representative immunoblots of HGF in livers from HGF<sup>ΔLSEC</sup> and control mice at different time points after PH (n=3) **B.** Quantification of hepatic expression of the HGF/c-Met signalling pathway after 70% PH in HGF<sup>ΔLSEC</sup> and control mice. \*p < 0.05, \*\*p < 0.01, \*\*\*p < 0.001.

#### 4.8 Deptor protein is downregulated in HGF<sup>ALSEC</sup> mice after PH

To decipher additional pathways regulated by angiocrine HGF signalling in liver regeneration, RNA sequencing was performed on whole liver RNA at 0 and 48 h post PH (Figure 15). The expression of 17 genes was found to be differentially expressed between HGF<sup>ALSEC</sup> and control livers at 48 h after PH. Among these genes, Deptor was found to be downregulated in HGF<sup>ALSEC</sup> mice. Deptor (DEP-domain containing mTOR-interacting protein) is an inhibitor of mTOR, a serine/threonine kinase, known to regulate mRNA translation, autophagy, and cell survival.(Catena and Fanciulli 2017) Loss of Deptor has been shown to induce apoptosis through the downregulation of PI3K/AKT signalling.(Srinivas, Viji et al. 2016)

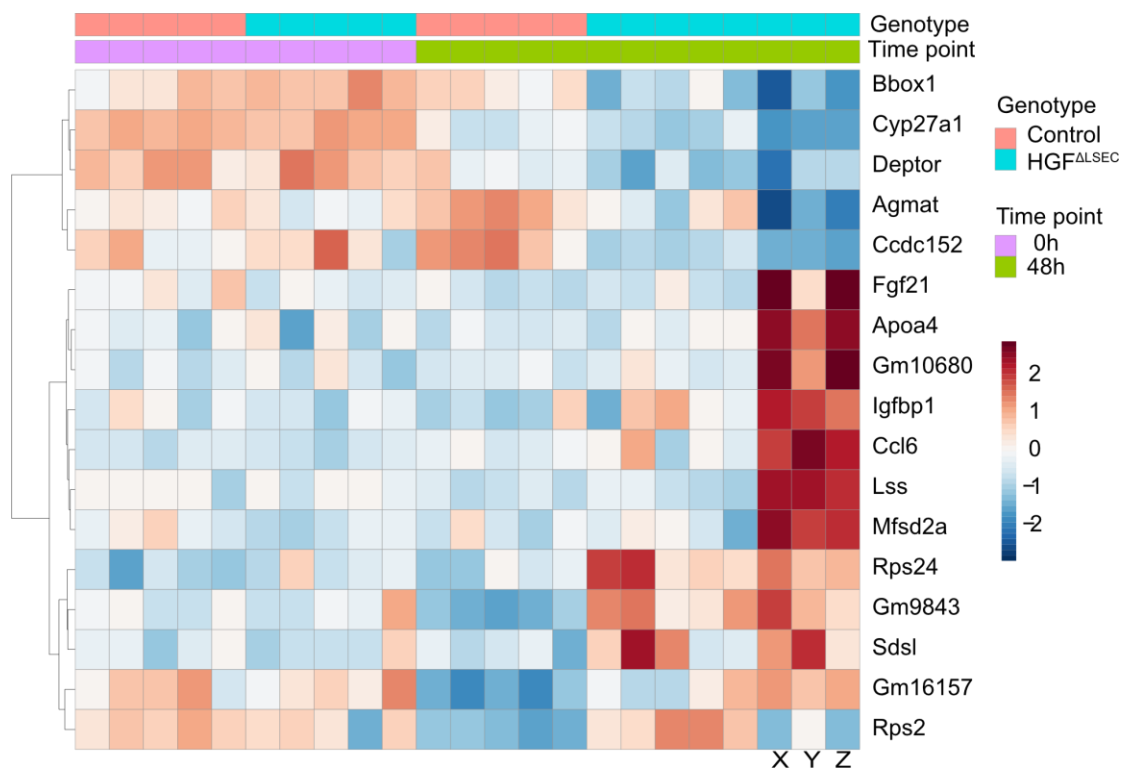


**Figure 15.** Heatmap of RNA-seq showing the expression of the 17 genes found to be differentially expressed in control livers compared to HGF<sup>ALSEC</sup> livers ( $n \geq 5$ ). Red corresponds to upregulated genes and blue corresponds to

downregulated genes. The colour scale represents the z-scaled gene expression levels.

The result of the RNA sequencing were confirmed at the protein level. Western blotting show that Deptor was downregulated in HGF $\Delta$ SEC mice compared to control mice 48 h after PH. (Figure 16A). A 4-fold reduction in hepatic Deptor at 48 h after PH in HGF $\Delta$ SEC mice was detected. (Figure 16B). Thus, Deptor is downregulated in HGF $\Delta$ SEC mice after PH at both the mRNA and protein level. Deptor is known to be a positive regulator of cell proliferation. Deptor can activate the Akt pathway in order to promote cellular proliferation and survival.

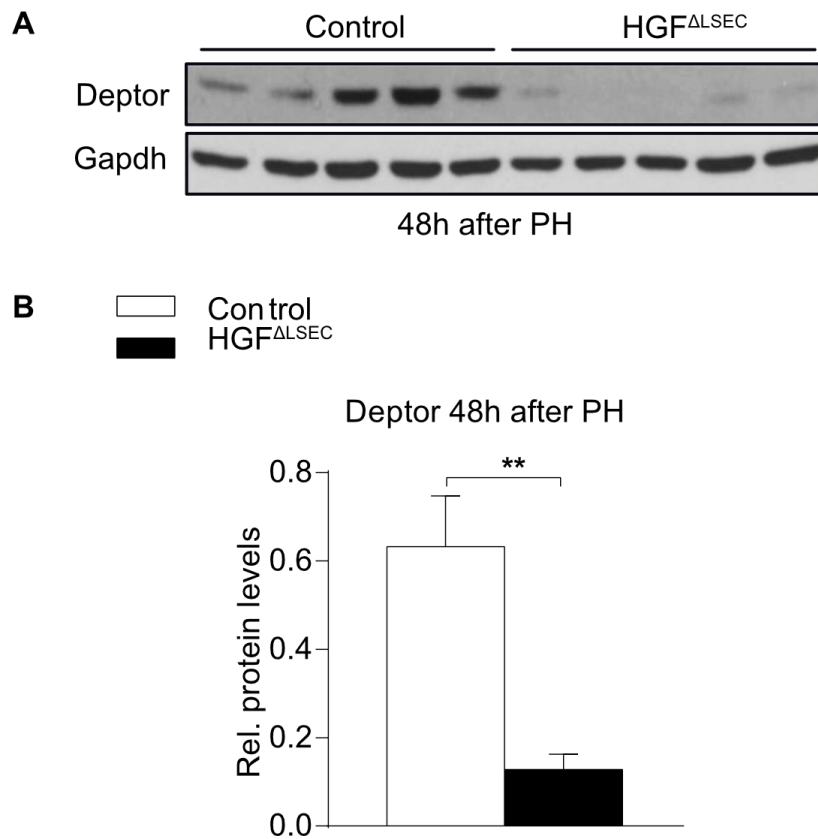


**Figure 16. A.** Immunoblots of HGF in livers of HGF $\Delta$ SEC and control mice at 48 h after PH (n=5). **B.** Downregulation of hepatic Deptor 48 h after PH in HGF $\Delta$ SEC compared to control mice (n=5). Results are represented as mean  $\pm$  S.E.M. \*\*p < 0.01.

# 5 Discussion

## 5.1 The generation of a new LSEC-specific HGF KO mouse model

HGF, its receptor c-Met, epidermal growth factor receptor (EGFR), and its ligands are different forms of complete mitogens.(Michalopoulos 2010) The HGF/c-Met axis is involved in the physiological homeostasis and regeneration of many extrahepatic organs such as the heart, kidney, lung, gut, and skin.(Nakamura and Mizuno 2010) It is known that HGF is essential for liver growth and organ regeneration. Several studies have shown that systematic ablation of HGF or its receptor c-Met in mice leads to abnormal liver development and lethality in utero.(Bladt, Riethmacher et al. 1995, Schmidt, Bladt et al. 1995, Uehara, Minowa et al. 1995) Different methods have been used to elucidate HGF/c-Met signalling during liver regeneration.(Phaneuf, Moscioni et al. 2004, Paranjpe, Bowen et al. 2007, Ishikawa, Factor et al. 2012, Nejak-Bowen, Orr et al. 2013)

Cre-loxP-mediated gene targeting technology has been used to generate hepatocyte-specific c-Met knock-out mice. Two independent studies found that these mice were viable but showed high mortality rates after PH.(Borowiak, Garratt et al. 2004, Huh, Factor et al. 2004) The suppression of HGF or c-Met by RNA interference in normal rats resulted in impaired proliferation kinetics of hepatocytes associated with liver regeneration.(Paranjpe, Bowen et al. 2007)

Recently, Cao and colleagues used an inducible LSEC-specific HGF knockout mouse model and found that deletion of HGF in mouse LSECs blocked regeneration and led to fibrosis.(Cao, Ye et al. 2017) LSECs are highly specialised capillary endothelial cells of the liver, which are not only passive conduits for delivering blood, but also play an important role in liver metabolism, growth, and regeneration.(DeLeve 2013, Rafii, Butler et al. 2016, Koch, Olsavszky et al. 2017, Leibing, Geraud et al. 2018) Although inducible endothelial cell-specific KO models are suitable for the analysis of transient effects of angiokine deprivation, constitutive knock-out models have proven

effective to better understand the impact on development or long-term homeostasis. To exemplify, induced conditional deletion of the wnt cargo receptor Evi (Wls) in VE-Cadherin-positive endothelial cells of adult mice resulted in decreased proliferation and expression of GS and Axin2 in pericentral hepatocytes with no developmental differences.(Wang, Zhao et al. 2015)

By using the LSEC subtype-specific Stab2-Cre mice to delete Wls, Leibing et al. have shown that constitutive loss of angiocrine wnt signalling also leads to a reduced number of offspring, diminished body weight, lower liver-to-body weight ratio, and lower plasma cholesterol levels.(Leibing, Geraud et al. 2018) Similarly, developmental or metabolic changes have not been described in a tamoxifen-inducible deletion of HGF in VE-Cadherin-positive endothelial cells.(Cao, Ye et al. 2017) In the present study, we used a new HGF<sup>ΔLSEC</sup> mouse model, which was generated by our collaborator at University Medical Center and Medical Faculty Mannheim, Heidelberg University. In HGF<sup>ΔLSEC</sup> mice, HGF is knocked out LSEC-specifically as early as during embryonic development. Here, we show for the first time that angiocrine HGF signalling does not affect liver metabolism under steady-state conditions, but leads to a reduced body, liver, and spleen weight.

## **5.2 Ablation of HGF in LSECs results in lower body weight but normal liver development and function**

HGF is essential for liver development. Livers of global HGF KO mice were severely reduced in size from E12.5 and this reduction was more pronounced at E14.5.(Schmidt, Bladt et al. 1995) HGF<sup>ΔLSEC</sup> mice showed reduced body weight in both sexes but the same liver-to-body weight ratio. Liver weight was significantly lower in females and had a tendency to be lower in male mice. Similarly, spleen weight was significantly lower in males and had a tendency to be lower in female mice. These results indicate that HGF<sup>ΔLSEC</sup> mice are a little smaller at 9 weeks old than control mice. The significant reduction in liver weight in HGF<sup>ΔLSEC</sup> mice indicates that angiocrine HGF signalling plays an

important role in liver development. This is due to the fact that the liver performs a multitude of essential functions for the whole body and plays a vital role in the regulation of metabolism in tissues.(Michalopoulos 2013) As a consequence, a small liver probably leads to the reduction in body weight of HGF<sup>ΔLSEC</sup> mice.

Histology of HGF<sup>ΔLSEC</sup> mice did not reveal significant morphological changes, inflammation, or depositions of polysaccharides or collagens according to H&E, PAS, and Sirius Red. Therefore, except for being slightly but significantly lighter, HGF<sup>ΔLSEC</sup> did not show major alterations in liver development or function or any general impairment.

### **5.3 Ablation of HGF in LSECs suppresses liver regeneration at the early stage after PH**

The liver is the only solid organ in mammals that can regenerate after hepatectomy. In this study, a 70% PH mouse model was employed.(Mitchell and Willenbring 2008) After 70% PH, the residual liver is able to regenerate and restore its original mass within 7 d.(Michalopoulos 2017) Intriguingly, HGF<sup>ΔLSEC</sup> mice show an impaired liver regeneration and a reduced liver-to-body-weight ratio at 72 h after PH, despite that fact that both hepatic stellate cells (HSC) and LSEC contribute to the increase in HGF production after PH.(Michalopoulos 2010, Michalopoulos 2013) The impaired liver-to-body weight ratio was restored to normal at 96 h after PH (Figure 8). Furthermore, the changes in liver-to-body weight ratio reduced hepatic proliferation. Despite the proliferation peaks at 48 h after PH in our experiment, we did not notice a reduced liver-to-body-weight ratio at the 48 h time point. Hypertrophy of hepatocytes after PH might be the reason.

The proliferation of hepatocytes, which can be investigated using both BrdU and Ki67 staining, reached a peak at approximately 48 h and terminated at 168 h after PH in control mice (Figure 9A and 9B; Figure 10A and 10B). Interestingly, HGF<sup>ΔLSEC</sup> hepatocytes showed reduced proliferation rates at 48

h after PH compared to control mice, whereas from 72 to 168 h, there was no significant difference between the two groups. Ki67 staining usually shows a higher percentage of positive hepatocytes than BrdU staining. At 48 h after PH, the percentage of BrdU-positive hepatocytes is around 20%, while Ki67-positive hepatocytes is around 50%. The reason of the difference is that BrdU can be incorporated into the newly synthesised DNA of replicating cells during the S phase of the cell cycle, but Ki67 protein is present during all active phases of the cell cycle (G1, S, G2, and M), but absent in quiescent cells (G0). (Bruno and Darzynkiewicz 1992)

Borowiak and colleagues (Borowiak, Garratt et al. 2004) observed that BrdU-positive cells were decreased by 60% in hepatocyte-specific c-Met knock-out mice compared to control mice after PH. A similar reduction was seen for Ki67-positive cells. In the present study, a 48% reduction in BrdU-positive hepatocytes was observed in HGF<sup>ΔLSEC</sup> mice compared to control mice; similarly a 45% reduction in Ki67-positive hepatocytes was observed. Cao et al. also found that hepatocyte proliferation was lower in the inducible LSEC-specific HGF knockout mouse model than in controls, as determined by qualitative immunostaining. (Cao, Ye et al. 2017) Both of these findings are similar to our research results.

It seems that ablation of HGF in LSECs only suppresses liver regeneration at the early stages after PH. Many cytokines and growth factors, e.g. HGF, the EGF family, FGFs, VEGF, IGFs, etc., are involved in liver regeneration. (Bohm, Kohler et al. 2010) Ablation of one of these cytokines and growth factors might impair but not diminish the regeneration of the liver. Other signals might compensate for the mitogenic function of HGF in HGF<sup>ΔLSEC</sup> mice. As a result, we did not observe a difference in either hepatocyte proliferation or the liver-to-body weight ratio after 72 h.

#### **5.4 The mechanisms of impaired liver regeneration in HGF<sup>ΔLSEC</sup> mice**

HGF is known to serve as a major hepatocyte mitogen, which performs its

activity through activation of the receptor tyrosine kinase c-Met. HGF expression is known to be upregulated in the liver after PH.(Michalopoulos 2007) After PH, HGF not only rises in liver tissue, but also in lung,(Yanagita, Nagaike et al. 1992) spleen, and kidney tissue.(Kono, Nagaike et al. 1992) This phenomenon might play an important role even though its relationship with PH is not clear.

Compared to the sham-operation group, phosphorylation of c-Met was significantly upregulated by 3.5-fold at 5 min and by 8-fold at 60 min after PH in rats.(Stolz, Mars et al. 1999) Intriguingly, the HGF/c-Met signalling pathway was downregulated in the HGF<sup>ΔLSEC</sup> group after PH. HGF mRNA expression (at 12 h) and HGF protein expression (at 48 and 72 h) were significantly decreased in HGF<sup>ΔLSEC</sup> mice compared to control mice after PH. Consistent with the HGF level, phosphorylation of c-Met (at 48 h) was also decreased. However, there was no difference in HGF protein expression between HGF<sup>ΔLSEC</sup> and control mouse livers before PH.

There are two phases in the expression of endogenous HGF. In the consumptive phase (from 0 to 3 h), HGF levels decrease and are used in part from hepatic stores. In the productive phase (from 3 to 72 h) HGF levels increase.(Pediaditakis, Lopez-Talavera et al. 2001) Since inactive HGF stored in the liver matrix is not enough to promote hepatocyte proliferation and HGF-derived from LSECs is not completely compensated for by other growth factors and cytokines, our results confirmed the vital role of hepatic angiocrine HGF signalling in the early stages of liver regeneration after PH.

The present study aimed to elucidate the angiocrine HGF signalling mechanisms in liver regeneration. RNA sequencing revealed a wide spectrum of possibly related genes. Overall, Deptor was found to show the strongest downregulation in mRNA levels of all the differentially expressed genes in HGF<sup>ΔLSEC</sup> livers compared to control livers. Deptor has been described as an mTOR-interacting protein that regulates several molecular pathways, such as cell growth, apoptosis, and autophagy.(Peterson, Laplante et al. 2009, Zhang, Chen et al. 2013, Zhang, Chen et al. 2013, Catena and Fanciulli 2017) Deptor

is also known to be a positive regulator of cell proliferation. Deptor overexpression can inhibit mTORC1 and leads to an increase in mTORC2 signalling, thus leading to Akt phosphorylation. This effect is induced by PI3K, the major upstream regulator of Akt.(Peterson, Laplante et al. 2009)

Furthermore, the absence of Deptor has been shown to stimulate caspase-dependent apoptosis.(Srinivas, Viji et al. 2016, Catena and Fanciulli 2017) Interestingly, Deptor protein levels were found to be lower in HGF<sup>ΔSEC</sup> mice than control mice at 48 h after PH, which is consistent with the appearance of liver necrosis in HGF<sup>ΔSEC</sup> mice. Liver necrosis was observed 48 to 96 h after PH, with no necrosis present in the livers of control hepatectomised mice.

IGFBP-1 is one of the strongest upregulated genes in HGF<sup>ΔSEC</sup> livers 48 h after PH. IGFBP-1 protein has been found to specifically bind to and modulate the bioavailability of insulin-like growth factors (IGF-I and IGF-II), which are known to be involved in liver regeneration. IGFBP-1 KO mice demonstrated impaired liver regeneration after PH, characterised by liver necrosis and reduced and delayed hepatocyte proliferation.(Leu, Crissey et al. 2003) Thus, upregulation of IGFBP-1 in HGF<sup>ΔSEC</sup> livers could be a compensatory response to stimulate liver regeneration after PH.

### **5.5 Liver necrosis after PH in HGF<sup>ΔSEC</sup> mice**

Liver necrosis after PH has also been previously described by other groups studying liver regeneration after ablation of the c-Met gene in adult mouse hepatocytes.(Borowiak, Garratt et al. 2004, Huh, Factor et al. 2004) Huh et al. observed a lethality of approximately 80% in hepatocyte-specific c-Met KO mice 48 h after PH, with numerous areas of necrosis.(Huh, Factor et al. 2004) Borowiak et al. found that if a transverse incision below the rib cage was used for PH, 95% of conditional Met mutant mice died within 2 to 3 d after PH. However, when using a longitudinal incision, 85% of conditional Met mutant mice survived.(Borowiak, Garratt et al. 2004) In our study, 15% to 35% of necrotic areas was seen in up to 40% of HGF<sup>ΔSEC</sup> mice at 48 to 96 h after PH,

whereas predefined euthanasia endpoints were observed only in 12.8% HGF<sup>ΔLSEC</sup> mice from 48 to 72 h after PH in this study (Figure 11A and 11B). Liver necrosis and lethality are probably a consequence of loss of liver function and liver failure due to impaired liver regeneration. Accordingly, HGF<sup>ΔLSEC</sup> mice showed increased ALT levels at 48 and 168 h after PH (Figure 12). These results indicate that angiocrine HGF prevents liver damage after injury through Deptor, an anti-apoptotic agent.

## 5.6 LSEC and liver regeneration

LSECs are special endothelial cells that intersperse the surface of liver sinusoids, separating the blood cells on one side and hepatocytes and hepatic stellate cells (HSC) on the other side.(Poisson, Lemoinne et al. 2017) Under normal conditions, HSC are the main source of HGF. However, after liver injury, LSECs play a more important role in HGF expression.(DeLeve 2013) LSECs are regarded as one of the most important liver cell types that produce HGF during liver regeneration.(DeLeve 2013, Poisson, Lemoinne et al. 2017) Previous studies have confirmed that LSEC can produce HGF and are involved in liver regeneration following PH.(Ding, Nolan et al. 2010) Nevertheless, the exact contribution of HGF produced by LSECs during liver regeneration remains to be identified.

Up until now, there has been no unique marker for LSECs. Usually a combination of markers are needed to identify LSECs. But some markers of LSECs, such as CD31 or CD45, are being controversially discussed.(Poisson, Lemoinne et al. 2017) Several LSECs isolation protocols have been established.(Meyer, Lacotte et al. 2016, Liu, Huang et al. 2017) Although it is difficult to establish a culture of primary LSECs, several methods can be used to improve LSECs culture. For example, co-culture with hepatocytes and fibroblasts,(March, Hui et al. 2009), the addition of VEGF to the medium(Yokomori, Oda et al. 2003) and the use of 5% oxygen.(Martinez, Nedredal et al. 2008) Several immortalised LSEC lines have been developed(Poisson, Lemoinne et al. 2017).

In the present study, we used a new HGF<sup>ΔSEC</sup> mouse model that allows us to explore the angiocrine HGF signalling during liver regeneration. PH was performed on HGF<sup>ΔSEC</sup> mice and compared to control mice. The impaired liver regeneration and downregulation of the HGF/c-Met signalling pathway in HGF<sup>ΔSEC</sup> mice suggests that angiocrine HGF signalling plays a vital role in hepatocyte proliferation during liver regeneration.

## 6 Summary

In this project, we analysed a new LSEC-specific HGF-KO ( $\text{HGF}^{\Delta\text{LSEC}}$ ) in mice that is active from early foetal development onwards. This model, therefore, enables a comprehensive investigation of angiocrine HGF signalling during liver development as well as in physiological homeostasis and regeneration during adulthood. Angiocrine HGF signalling does not affect liver metabolism under steady-state conditions, but leads to a reduction in body, liver, and spleen weight. We have observed that  $\text{HGF}^{\Delta\text{LSEC}}$  mice show an impaired liver regeneration and a reduced liver-to-body-weight ratio compared to control mice at 72 h after PH. The HGF/c-MET signalling pathway was found to be less active in  $\text{HGF}^{\Delta\text{LSEC}}$  and an impaired activation of this axis involved the downregulation of the anti-apoptotic protein Deptor, representing a novel target of this signalling pathway in this context. Angiocrine HGF signalling is not only essential for liver regeneration and preventing liver damage after injury, but is also essential for the growth of the whole organism.

## 7 Abbreviations

CCI4	Carbon tetrachloride
BrdU	Bromodeoxyuridine
DNA	Deoxyribonucleic acid
EGF	Epidermal growth factor
ELISA	Enzyme-linked immunosorbent assay
FGF	Fibroblast growth factor
GAPDH	Glyceraldehyde 3-phosphate dehydrogenase
H&E	Hematoxylin & eosin
HGF	Hepatocyte growth factor
HSC	Hepatic stellate cells
IGF	Insulin-like growth factor
IL	Interleukin
KO	Knock out
LSEC	Liver sinusoid endothelial cell
mRNA	Messenger ribonucleic acid
mTOR	Mammalian target Of Rapamicin
PBS	Phosphate buffered saline
PCR	Polymerase chain reaction

PFA	Paraformaldehyde
PH	Partial hepatectomy
qRT-PCR	Quantitative reverse-transcription PCR
RNA	Ribonucleic acid
SDS-PAGE	SDS-polyacrylamide gel electrophoresis
SPF	Specific-pathogen-free
Stab2	Stabilin-2
TBS	Tris-buffered saline
TEMED	Tetramethylethylenediamine
TGF	Transforming growth factor
TNF	Tumor necrosis factor

# 8 Figures and tables

## 8.1 Figures

Figure 1. Liver lobes and segments.(Liau, Blumgart et al. 2004). .....	8
Figure 2. The structure of the liver.(Si-Tayeb, Lemaigre et al. 2010) .....	9
Figure 3. Regulation of the G1/S transition.(Sherr and Roberts 1999) .....	13
Figure 4. Signalling interactions between different hepatic cell types during liver regeneration. (Michalopoulos 2007). .....	15
Figure 5. Pictures of control and HGF <sup>ΔSEC</sup> mice. The control mouse on the left and HGF <sup>ΔSEC</sup> mice on the right.....	42
Figure 6. Total body weight, liver weight, liver-to-body weight ratio, spleen weight and spleen-to-body weight of the mice. ....	44
Figure 7. H&E, PAS, and Sirius Red staining of liver from HGF <sup>ΔSEC</sup> mice compared to controls (male).. ..	44
Figure 8. Liver-to-body weight ratio of HGF <sup>ΔSEC</sup> and control mice at different time points after 70% PH.. ..	45
Figure 9. BrdU and Ki67 stainings of liver sections.. ..	46
Figure 10. Quantification of BrdU and Ki67 positive hepatocytes. ....	48
Figure 11. H&E staining of liver sections show necrotic areas.....	51
Figure 12. ALT activity of serum from HGF <sup>ΔSEC</sup> and control mice.....	53

Figure 13. qRT-PCR of HGF in livers of HGF $\Delta$ LSEC and control mice.....54

Figure 14. Hepatic expression of the HGF/c-Met signalling pathway after 70% PH.....56

Figure 15. Heatmap of RNA-seq. ....57

## 8.2 Tables

Table 1. Mouse lethality after partial hepatectomy within 168h.....49

Table 2. Numbers of mice with liver necrosis at different time points after partial hepatectomy.....50

## 9 References

Basilico, C., A. Arnesano, M. Galluzzo, P. M. Comoglio and P. Michieli (2008). "A high affinity hepatocyte growth factor-binding site in the immunoglobulin-like region of met." Journal of Biological Chemistry **283**(30): 21267-21277.

Bell, A. W., J. G. Jiang, Q. Chen, Y. Liu and R. Zarnegar (1998). "The upstream regulatory regions of the hepatocyte growth factor gene promoter are essential for its expression in transgenic mice." J Biol Chem **273**(12): 6900-6908.

Bladt, F., D. Riethmacher, S. Isenmann, A. Aguzzi and C. Birchmeier (1995). "Essential Role for the C-Met Receptor in the Migration of Myogenic Precursor Cells into the Limb Bud." Nature **376**(6543): 768-771.

Blouin, A., R. P. Bolender and E. R. Weibel (1977). "Distribution of organelles and membranes between hepatocytes and nonhepatocytes in the rat liver parenchyma. A stereological study." J Cell Biol **72**(2): 441-455.

Bohm, F., U. A. Kohler, T. Speicher and S. Werner (2010). "Regulation of liver regeneration by growth factors and cytokines." EMBO Mol Med **2**(8): 294-305.

Borowiak, M., A. N. Garratt, T. Wustefeld, M. Strehle, C. Trautwein and C. Birchmeier (2004). "Met provides essential signals for liver regeneration." Proc Natl Acad Sci U S A **101**(29): 10608-10613.

Bruno, S. and Z. Darzynkiewicz (1992). "Cell-Cycle Dependent Expression and Stability of the Nuclear-Protein Detected by Ki-67 Antibody in HI-60 Cells." Cell Proliferation **25**(1): 31-40.

Cao, Z., T. Ye, Y. Sun, G. Ji, K. Shido, Y. Chen, L. Luo, F. Na, X. Li, Z. Huang, J. L. Ko, V. Mittal, L. Qiao, C. Chen, F. J. Martinez, S. Rafii and B. S. Ding (2017).

"Targeting the vascular and perivascular niches as a regenerative therapy for lung and liver fibrosis." Sci Transl Med **9**(405).

Catena, V. and M. Fanciulli (2017). "Deptor: not only a mTOR inhibitor." J Exp Clin Cancer Res **36**(1): 12.

Cheng, Z., L. Liu, X. J. Zhang, M. Lu, Y. Wang, V. Assfalg, M. Laschinger, G. von Figura, Y. Sunami, C. W. Michalski, J. Kleeff, H. Friess, D. Hartmann and N. Huser (2018). "Peroxisome Proliferator-Activated Receptor gamma negatively regulates liver regeneration after partial hepatectomy via the HGF/c-Met/ERK1/2 pathways." Sci Rep **8**(1): 11894.

Clavien, P. A., H. Petrowsky, M. L. DeOliveira and R. Graf (2007). "Strategies for safer liver surgery and partial liver transplantation." N Engl J Med **356**(15): 1545-1559.

Costa, R. H., V. V. Kalinichenko, A. X. L. Holterman and X. H. Wang (2003). "Transcription factors in liver development, differentiation, and regeneration." Hepatology **38**(6): 1331-1347.

DeLeve, L. D. (2013). "Liver sinusoidal endothelial cells and liver regeneration." J Clin Invest **123**(5): 1861-1866.

Ding, B. S., D. J. Nolan, J. M. Butler, D. James, A. O. Babazadeh, Z. Rosenwaks, V. Mittal, H. Kobayashi, K. Shido, D. Lyden, T. N. Sato, S. Y. Rabbany and S. Rafii (2010). "Inductive angiocrine signals from sinusoidal endothelium are required for liver regeneration." Nature **468**(7321): 310-315.

Eipel, C., K. Abshagen and B. Vollmar (2010). "Regulation of hepatic blood flow: The hepatic arterial buffer response revisited." World Journal of Gastroenterology **16**(48): 6046-6057.

Fajardo-Puerta, A. B., M. Mato Prado, A. E. Frampton and L. R. Jiao (2016). "Gene of the month: HGF." J Clin Pathol **69**(7): 575-579.

Gebhardt, R., A. Baldysiak-Figiel, V. Krugel, E. Ueberham and F. Gaunitz (2007). "Hepatocellular expression of glutamine synthetase: An indicator of morphogen actions as master regulators of zonation in adult liver." Progress in Histochemistry and Cytochemistry **41**(4): 201-266.

Geraud, C., P. S. Koch, J. Zierow, K. Klapproth, K. Busch, V. Olsavszky, T. Leibing, A. Demory, F. Ulbrich, M. Dieltz, S. Singh, C. Sticht, K. Breitkopf-Heinlein, K. Richter, S. M. Karppinen, T. Pihlajaniemi, B. Arnold, H. R. Rodewald, H. G. Augustin, K. Schledzewski and S. Goerdts (2017). "GATA4-dependent organ-specific endothelial differentiation controls liver development and embryonic hematopoiesis." J Clin Invest **127**(3): 1099-1114.

Giordano, S. and A. Columbano (2014). "Met as a therapeutic target in HCC: facts and hopes." J Hepatol **60**(2): 442-452.

Haga, S., W. Ogawa, H. Inoue, K. Terui, T. Ogino, R. Igarashi, K. Takeda, S. Akira, S. Enosawa, H. Furukawa, S. Todo and M. Ozaki (2005). "Compensatory recovery of liver mass by Akt-mediated hepatocellular hypertrophy in liver-specific STAT3-deficient mice." J Hepatol **43**(5): 799-807.

Haga, S., M. Ozaki, H. Inoue, Y. Okamoto, W. Ogawa, K. Takeda, S. Akira and S. Todo (2009). "The survival pathways phosphatidylinositol-3 kinase (PI3-K)/phosphoinositide-dependent protein kinase 1 (PDK1)/Akt modulate liver

regeneration through hepatocyte size rather than proliferation." Hepatology **49**(1): 204-214.

Huh, C. G., V. M. Factor, A. Sanchez, K. Uchida, E. A. Conner and S. S. Thorgeirsson (2004). "Hepatocyte growth factor/c-met signaling pathway is required for efficient liver regeneration and repair." Proc Natl Acad Sci U S A **101**(13): 4477-4482.

Ishikawa, T., V. M. Factor, J. U. Marquardt, C. Raggi, D. Seo, M. Kitade, E. A. Conner and S. S. Thorgeirsson (2012). "Hepatocyte growth factor/c-met signaling is required for stem-cell-mediated liver regeneration in mice." Hepatology **55**(4): 1215-1226.

Koch, P. S., V. Olsavszky, F. Ulbrich, C. Sticht, A. Demory, T. Leibing, T. Henzler, M. Meyer, J. Zierow, S. Schneider, K. Breitkopf-Heinlein, H. Gaitantzi, B. Spencer-Dene, B. Arnold, K. Klapproth, K. Schledzewski, S. Goerdts and C. Geraud (2017). "Angiocrine Bmp2 signaling in murine liver controls normal iron homeostasis." Blood **129**(4): 415-419.

Kono, S., M. Nagaike, K. Matsumoto and T. Nakamura (1992). "Marked induction of hepatocyte growth factor mRNA in intact kidney and spleen in response to injury of distant organs." Biochem Biophys Res Commun **186**(2): 991-998.

LeCouter, J., D. R. Moritz, B. Li, G. L. Phillips, X. H. Liang, H. P. Gerber, K. J. Hillan and N. Ferrara (2003). "Angiogenesis-independent endothelial protection of liver: role of VEGFR-1." Science **299**(5608): 890-893.

Leibing, T., C. Geraud, I. Augustin, M. Boutros, H. G. Augustin, J. G. Okun, C. D. Langhans, J. Zierow, S. A. Wohlfeil, V. Olsavszky, K. Schledzewski, S.

Goerdts and P. S. Koch (2018). "Angiocrine Wnt signaling controls liver growth and metabolic maturation in mice." Hepatology **68**(2): 707-722.

Leu, J. I., M. A. Crissey, L. E. Craig and R. Taub (2003). "Impaired hepatocyte DNA synthetic response posthepatectomy in insulin-like growth factor binding protein 1-deficient mice with defects in C/EBP beta and mitogen-activated protein kinase/extracellular signal-regulated kinase regulation." Mol Cell Biol **23**(4): 1251-1259.

Liau, K. H., L. H. Blumgart and R. P. DeMatteo (2004). "Segment-oriented approach to liver resection." Surgical Clinics of North America **84**(2): 543-+.

Liau, K. H., L. H. Blumgart and R. P. DeMatteo (2004). "Segment-oriented approach to liver resection." Surg Clin North Am **84**(2): 543-561.

Lindroos, P. M., R. Zarnegar and G. K. Michalopoulos (1991). "Hepatocyte Growth-Factor (Hepatopoietin-a) Rapidly Increases in Plasma before DNA-Synthesis and Liver-Regeneration Stimulated by Partial-Hepatectomy and Carbon-Tetrachloride Administration." Hepatology **13**(4): 743-750.

Lindroos, P. M., R. Zarnegar and G. K. Michalopoulos (1991). "Hepatocyte growth factor (hepatopoietin A) rapidly increases in plasma before DNA synthesis and liver regeneration stimulated by partial hepatectomy and carbon tetrachloride administration." Hepatology **13**(4): 743-750.

Liu, J., X. Huang, M. Werner, R. Broering, D. Yang and M. Lu (2017). "Advanced Method for Isolation of Mouse Hepatocytes, Liver Sinusoidal Endothelial Cells, and Kupffer Cells." Methods Mol Biol **1540**: 249-258.

Maher, J. J. (1993). "Cell-specific expression of hepatocyte growth factor in liver. Upregulation in sinusoidal endothelial cells after carbon tetrachloride." J Clin Invest **91**(5): 2244-2252.

March, S., E. E. Hui, G. H. Underhill, S. Khetani and S. N. Bhatia (2009). "Microenvironmental regulation of the sinusoidal endothelial cell phenotype in vitro." Hepatology **50**(3): 920-928.

Martinez, I., G. I. Nedredal, C. I. Oie, A. Warren, O. Johansen, D. G. Le Couteur and B. Smedsrod (2008). "The influence of oxygen tension on the structure and function of isolated liver sinusoidal endothelial cells." Comp Hepatol **7**: 4.

Meyer, J., S. Lacotte, P. Morel, C. Gonelle-Gispert and L. Buhler (2016). "An optimized method for mouse liver sinusoidal endothelial cell isolation." Exp Cell Res **349**(2): 291-301.

Michalopoulos, G. K. (2007). "Liver regeneration." J Cell Physiol **213**(2): 286-300.

Michalopoulos, G. K. (2010). "Liver regeneration after partial hepatectomy: critical analysis of mechanistic dilemmas." Am J Pathol **176**(1): 2-13.

Michalopoulos, G. K. (2013). "Principles of liver regeneration and growth homeostasis." Compr Physiol **3**(1): 485-513.

Michalopoulos, G. K. (2014). "Advances in liver regeneration." Expert Rev Gastroenterol Hepatol **8**(8): 897-907.

Michalopoulos, G. K. (2017). "Hepatostat: Liver regeneration and normal liver tissue maintenance." Hepatology **65**(4): 1384-1392.

Michalopoulos, G. K. and Z. Khan (2015). "Liver Stem Cells: Experimental Findings and Implications for Human Liver Disease." Gastroenterology **149**(4): 876-882.

Migliore, C. and S. Giordano (2008). "Molecular cancer therapy: can our expectation be MET?" Eur J Cancer **44**(5): 641-651.

Mitchell, C., M. Nivison, L. F. Jackson, R. Fox, D. C. Lee, J. S. Campbell and N. Fausto (2005). "Heparin-binding epidermal growth factor-like growth factor links hepatocyte priming with cell cycle progression during liver regeneration." Journal of Biological Chemistry **280**(4): 2562-2568.

Mitchell, C. and H. Willenbring (2008). "A reproducible and well-tolerated method for 2/3 partial hepatectomy in mice." Nat Protoc **3**(7): 1167-1170.

Miyaoka, Y., K. Ebato, H. Kato, S. Arakawa, S. Shimizu and A. Miyajima (2012). "Hypertrophy and unconventional cell division of hepatocytes underlie liver regeneration." Curr Biol **22**(13): 1166-1175.

Nakamura, T. and S. Mizuno (2010). "The discovery of Hepatocyte Growth Factor (HGF) and its significance for cell biology, life sciences and clinical medicine." Proceedings of the Japan Academy Series B-Physical and Biological Sciences **86**(6): 588-610.

Nakamura, T., K. Nawa and A. Ichihara (1984). "Partial purification and characterization of hepatocyte growth factor from serum of hepatectomized rats." Biochem Biophys Res Commun **122**(3): 1450-1459.

Nakamura, T., T. Nishizawa, M. Hagiya, T. Seki, M. Shimonishi, A. Sugimura, K. Tashiro and S. Shimizu (1989). "Molecular cloning and expression of human hepatocyte growth factor." Nature **342**(6248): 440-443.

Nejak-Bowen, K., A. Orr, W. C. Bowen, Jr. and G. K. Michalopoulos (2013). "Conditional genetic elimination of hepatocyte growth factor in mice compromises liver regeneration after partial hepatectomy." PLoS One **8**(3): e59836.

Noji, S., K. Tashiro, E. Koyama, T. Nohno, K. Ohyama, S. Taniguchi and T. Nakamura (1990). "Expression of hepatocyte growth factor gene in endothelial and Kupffer cells of damaged rat livers, as revealed by in situ hybridization." Biochem Biophys Res Commun **173**(1): 42-47.

Organ, S. L. and M. S. Tsao (2011). "An overview of the c-MET signaling pathway." Ther Adv Med Oncol **3**(1 Suppl): S7-S19.

Paranjpe, S., W. C. Bowen, A. W. Bell, K. Nejak-Bowen, J. H. Luo and G. K. Michalopoulos (2007). "Cell cycle effects resulting from inhibition of hepatocyte growth factor and its receptor c-met in regenerating rat livers by RNA interference." Hepatology **45**(6): 1471-1477.

Pediaditakis, P., J. C. Lopez-Talavera, B. Petersen, S. P. Monga and G. K. Michalopoulos (2001). "The processing and utilization of hepatocyte growth factor/scatter factor following partial hepatectomy in the rat." Hepatology **34**(4 Pt 1): 688-693.

Peterson, T. R., M. Laplante, C. C. Thoreen, Y. Sancak, S. A. Kang, W. M. Kuehl, N. S. Gray and D. M. Sabatini (2009). "DEPTOR Is an mTOR Inhibitor

Frequently Overexpressed in Multiple Myeloma Cells and Required for Their Survival." Cell **137**(5): 873-886.

Phaneuf, D., A. D. Mosconi, C. LeClair, S. E. Raper and J. M. Wilson (2004). "Generation of a mouse expressing a conditional knockout of the hepatocyte growth factor gene: demonstration of impaired liver regeneration." DNA Cell Biol **23**(9): 592-603.

Poisson, J., S. Lemoine, C. Boulanger, F. Durand, R. Moreau, D. Valla and P. E. Rautou (2017). "Liver sinusoidal endothelial cells: Physiology and role in liver diseases." J Hepatol **66**(1): 212-227.

Prati, D., E. Taioli, A. Zanella, E. Della Torre, S. Butelli, E. Del Vecchio, L. Vianello, F. Zanuso, F. Mozzi, S. Milani, D. Conte, M. Colombo and G. Sirchia (2002). "Updated definitions of healthy ranges for serum alanine aminotransferase levels." Annals of Internal Medicine **137**(1): 1-9.

Pratt, D. S. and M. M. Kaplan (2000). "Primary care: Evaluation of abnormal liver-enzyme results in asymptomatic patients." New England Journal of Medicine **342**(17): 1266-1271.

Rafii, S., J. M. Butler and B. S. Ding (2016). "Angiocrine functions of organ-specific endothelial cells." Nature **529**(7586): 316-325.

Russell, W. E., J. A. McGowan and N. L. Bucher (1984). "Partial characterization of a hepatocyte growth factor from rat platelets." J Cell Physiol **119**(2): 183-192.

Saxena, R., N. D. Theise and J. M. Crawford (1999). "Microanatomy of the human liver-exploring the hidden interfaces." Hepatology **30**(6): 1339-1346.

Schmidt, C., F. Bladt, S. Goedecke, V. Brinkmann, W. Zschiesche, M. Sharpe, E. Gherardi and C. Birchmeier (1995). "Scatter Factor/Hepatocyte Growth-Factor Is Essential for Liver Development." Nature **373**(6516): 699-702.

Schmidt, C., F. Bladt, S. Goedecke, V. Brinkmann, W. Zschiesche, M. Sharpe, E. Gherardi and C. Birchmeier (1995). "Scatter factor/hepatocyte growth factor is essential for liver development." Nature **373**(6516): 699-702.

Schulze, S., C. Stoss, M. Lu, B. Wang, M. Laschinger, K. Steiger, F. Altmayr, H. Friess, D. Hartmann, B. Holzmann and N. Huser (2018). "Cytosolic nucleic acid sensors of the innate immune system promote liver regeneration after partial hepatectomy." Sci Rep **8**(1): 12271.

Sherr, C. J. and J. M. Roberts (1999). "CDK inhibitors: positive and negative regulators of G1-phase progression." Genes Dev **13**(12): 1501-1512.

Si-Tayeb, K., F. P. Lemaigre and S. A. Duncan (2010). "Organogenesis and development of the liver." Dev Cell **18**(2): 175-189.

Srinivas, K. P., R. Viji, V. M. Dan, I. S. Sajitha, R. Prakash, P. V. Rahul, T. R. Santhoshkumar, S. Lakshmi and M. R. Pillai (2016). "DEPTOR promotes survival of cervical squamous cell carcinoma cells and its silencing induces apoptosis through downregulating PI3K/AKT and by up-regulating p38 MAP kinase." Oncotarget **7**(17): 24154-24171.

Stoker, M., E. Gherardi, M. Perryman and J. Gray (1987). "Scatter Factor Is a Fibroblast-Derived Modulator of Epithelial-Cell Mobility." Nature **327**(6119): 239-242.

Stolz, D. B., W. M. Mars, B. E. Petersen, T. H. Kim and G. K. Michalopoulos (1999). "Growth factor signal transduction immediately after two-thirds partial hepatectomy in the rat." Cancer Res **59**(16): 3954-3960.

Trusolino, L., A. Bertotti and P. M. Comoglio (2010). "MET signalling: principles and functions in development, organ regeneration and cancer." Nat Rev Mol Cell Biol **11**(12): 834-848.

Uehara, Y., O. Minowa, C. Mori, K. Shiota, J. Kuno, T. Noda and N. Kitamura (1995). "Placental defect and embryonic lethality in mice lacking hepatocyte growth factor/scatter factor." Nature **373**(6516): 702-705.

Wang, B., L. Zhao, M. Fish, C. Y. Logan and R. Nusse (2015). "Self-renewing diploid Axin2(+) cells fuel homeostatic renewal of the liver." Nature **524**(7564): 180-185.

Wang, B. C., B. Kaufmann, T. Engleitner, M. Lu, C. Mogler, V. Olsavszky, R. Ollinger, S. Y. Zhong, C. Geraud, Z. J. Cheng, R. R. Rad, R. M. Schmid, H. Friess, N. Huser, D. Hartmann and G. von Figura (2019). "Brg1 promotes liver regeneration after partial hepatectomy via regulation of cell cycle." Scientific Reports **9**.

Weidner, K. M., N. Arakaki, G. Hartmann, J. Vandekerckhove, S. Weingart, H. Rieder, C. Fonatsch, H. Tsubouchi, T. Hishida, Y. Daikuhara and et al. (1991). "Evidence for the identity of human scatter factor and human hepatocyte growth factor." Proc Natl Acad Sci U S A **88**(16): 7001-7005.

Yanagita, K., M. Nagaike, H. Ishibashi, Y. Niho, K. Matsumoto and T. Nakamura (1992). "Lung May Have an Endocrine Function Producing Hepatocyte Growth-

Factor in Response to Injury of Distal Organs." Biochemical and Biophysical Research Communications **182**(2): 802-809.

Yokomori, H., M. Oda, K. Yoshimura, T. Nagai, M. Ogi, M. Nomura and H. Ishii (2003). "Vascular endothelial growth factor increases fenestral permeability in hepatic sinusoidal endothelial cells." Liver Int **23**(6): 467-475.

Zarnegar, R., M. C. DeFrances, D. P. Kost, P. Lindroos and G. K. Michalopoulos (1991). "Expression of hepatocyte growth factor mRNA in regenerating rat liver after partial hepatectomy." Biochem Biophys Res Commun **177**(1): 559-565.

Zhang, H., J. Chen, Z. Zeng, W. Que and L. Zhou (2013). "Knockdown of DEPTOR induces apoptosis, increases chemosensitivity to doxorubicin and suppresses autophagy in RPMI-8226 human multiple myeloma cells in vitro." Int J Mol Med **31**(5): 1127-1134.

Zhang, H. R., J. M. Chen, Z. Y. Zeng and W. Z. Que (2013). "Knockdown of DEPTOR inhibits cell proliferation and increases chemosensitivity to melphalan in human multiple myeloma RPMI-8226 cells via inhibiting PI3K/AKT activity." J Int Med Res **41**(3): 584-595.

# 10 Curriculum vitae

**Name:** Xuejun Zhang

**Date of birth:** 01/12/1982

**Place of birth:** Jiangsu, China

**Nationality:** Chinese

**E-mail:** xuejun.zhang@tum.de

## University Education

06.2016 until now, doctoral candidate, TUM Medical Graduate Center, Technical University of Munich

09.2006-06.2009, master's degree of medicine, Graduate School of Clinical Medicine, Southeast University, Nanjing, China

09.2001-06.2006, bachelor's degree of medicine, School of Clinical Medicine, Southeast University, Nanjing, China

## Work Experience

10.2014-06.2016, attending physician, Department of Orthopedic Surgery, Zhongda Hospital, Southeast University

07.2009-09.2014, resident, Department of Orthopedics, Zhongda Hospital, Southeast University

## Publications

Cheng Z, Liu L, **Zhang XJ**, Lu M, Wang Y, Assfalg V, et al. Peroxisome Proliferator-Activated Receptor gamma negatively regulates liver regeneration after partial hepatectomy via the HGF/c-Met/ERK1/2 pathways. Sci Rep. 2018;8(1):11894.

Ji ML, Jiang H, **Zhang XJ**, Shi PL, Li C, Wu H, et al. Preclinical development of a microRNA-based therapy for intervertebral disc degeneration. *Nat Commun.* 2018;9(1):5051.

Lu J, Ji ML, **Zhang XJ**, Shi PL, Wu H, Wang C, et al. MicroRNA-218-5p as a Potential Target for the Treatment of Human Osteoarthritis. *Mol Ther.* 2017;25(12):2676-88.

Ji ML, **Zhang XJ**, Shi PL, Lu J, Wang SZ, Chang Q, et al. Downregulation of microRNA-193a-3p is involved in intervertebral disc degeneration by targeting MMP14. *J Mol Med (Berl).* 2016;94(4):457-68.

Ji ML, Lu J, Shi PL, **Zhang XJ**, Wang SZ, Chang Q, et al. Dysregulated miR-98 Contributes to Extracellular Matrix Degradation by Targeting IL-6/STAT3 Signaling Pathway in Human Intervertebral Disc Degeneration. *J Bone Miner Res.* 2016;31(4):900-9.

Hao ZC, Wang SZ, **Zhang XJ**, Lu J. Stem cell therapy: a promising biological strategy for tendon-bone healing after anterior cruciate ligament reconstruction. *Cell Prolif.* 2016;49(2):154-62.

# 11 Acknowledgements

I would like to deeply thank Univ.-Prof. Dr. Helmut Friess for accepting me as a medical graduate student at Technical University of Munich. I express my great gratitude for the opportunity to study in one of the most famous universities of the world.

I am most grateful to Prof. Dr. Norbert Hüser, who provided me with excellent supervision, continuous support, helpful discussions, kind assistance and good scientific environment.

I would like to express my gratitude to my mentor Dr. Dr. Daniel Hartmann. He not only provides a lot of supports for my research project, but also gives a lot of help to my family to solve many life problems which is difficult as foreigners.

I would like to express my gratitude to PD Dr. Guido von Figura for supervising the project and providing tremendous support for my research.

I would like to thank Cyrill Géraud, Victor Olsavszky and Kai Schledzewski of medical faculty Mannheim at Heidelberg University, and Thomas Engleitner, Rupert Öllinger, Roland Rad of II. Institute of Molecular Oncology and Functional Genomics at Technical University of Munich for their help of the research. They provide some experimental results for me.

I would like to thank my colleagues of the lab, Baocai Wang, Miao Lu, Yang Wang, Yuhan Yin, Alexandra Graupner, Suyang Zhong, and Ana Hidalgo.

I also would like to thank Prof. Dr. Bernhard Holzmann, PD Dr. rer. physiol. Melanie Laschinger and Prof. Dr. rer. nat Klaus-Peter Janssen for their kind supports during my work.

Finally, I am grateful to China Scholarship Council for funding parts of this study.